DYNAMIC ANALYSIS OF CAMS

Robert Viggo Andersen

United States
Naval Postgraduate School

THESIS

DYNAMIC ANALYSIS OF CAMS

by

Robert Viggo Andersen

June 1971

Dynamic Analysis of Cams

by

Robert Viggo Andersen
Lieutenant, United States Navy
B.S., United States Naval Academy, 1964

Submitted in partial fulfillment of the
requirements for the degree of

MASTER OF SCIENCE IN MECHANICAL ENGINEERING

from the

NAVAL POSTGRADUATE SCHOOL
June 1971

ABSTRACT

This thesis deals with the computer simulated, elastic link model of an automobile cam actuated valve train. Examined are the dynamic responses to such situations as: valve bounce, pushrod bounce, excessive cam speed, cam surface machining errors, and cam profiles. The model is adaptable to various types of mechanisms and lends itself well to the incorporation on a computer graphics display.

TABLE OF CONTENTS

3

LIST OF SYMBOLS

A	Area
[C]	System damping matrix
c_{ij}	Element of damping matrix
C_i	Constants
C_{Vi}, C_{Di}	Constants used in integration solution
E	Elastic modulus
F_i	External forces
$\{F_n\}$	Normalized force vector
g	Acceleration of gravity
h	Function used in integration solution
I	Moment of inertia
[K]	System stiffness matrix
k_{ij}	Element of stiffness matrix
L	Length
[M]	System mass matrix
M	Mass
m_{ij}	Elements of mass matrix
{P}	Force vector used in integration solution
q	System coordinate
r	Function used in integration solution
t	Time
ΔT	Time increment used in integration solution
T_i	Period
u	Element coordinate
$\{\alpha\}$	Vector used in integration solution

5

$[\beta]$	Transformation matrix
ζ	Damping coefficient
θ	Cam angle of rotation
$\{\phi\}$	Eigenvectors listed in columns, modal matrix
$\{\psi\}$	Vector used in integration solution
ω_n	Natural frequency

ACKNOWLEDGEMENTS

The author wishes to thank Professor R. C. Winfrey of the Naval
Postgraduate School for his constructive supervision and encouragement
throughout the work on this thesis.

I. INTRODUCTION

The study of cam actuated valve train mechanisms has been undertaken
in the last thirty years from many different approaches. The mechanism
has often been dissected to observe various local responses with the
remainder of the mechanism considered as external to the local point of
interest.

Some history of past work undertaken will help to demonstrate the
usefulness of the results to be presented later in this thesis.

Of basic interest to those dealing with valve train mechanisms
is what role does the cam profile play on the over-all response of the
system. Dudley [1], [2] examined the design of cam profile by use of the
valve output. This technique was carried out also by Thoren, Engemann,
and Stoddart [3] who included experimental results based on observations
of various engines and cam designs. More recent analysis has been done
by A. R. Johnson [4]. Johnson dealt with a numerical application of
Newton's Fundamental Interpolation Formula to look at a multi-degree of
freedom system. Again the idea was to take the desired output and relate
it in terms of the input. The above references are significant for they
reaffirm the importance of the output being a dominant factor to the design
of a cam.

Historically there has been a large amount of controversy over the
best cam for design purposes. Three types of cams: parabolic, harmonic,
and cycloidal often have been studied and compared to each other in terms
of displacement, velocity, acceleration, and jerk [5], [6], [7], [8], [9].

8

Polydyne cam profiles with their added flexibility have become popular. They can easily be adapted to sets of conditions which may be imposed by the mechanism [1], [2], [4], [10], [11], [12], [13], [14]. The problem here is that the cam may be over designed, in other words, it may be too exactly defined to be manufacturable.

In addition to those mentioned above, references [15], [16], and [17] present other methods of obtaining a cam profile. As can be seen there is a wealth of information to the cam designer to aid him in obtaining a cam profile, provided he has the necessary input data.

The ability to analyze a particular cam profile's effect on a system can be of great benefit. Experimental results are the best, but also the costliest. In addition, experimentation is best utilized if it can be compared with theoretical results. This can give indications of existing conditions which may not have been considered previously.

The ability to produce a model of a mechanism provides the chance to obtain a balance of varied information for analysis. Models have the same deficiencies as the human brain, i.e., they consider only a portion of the existing conditions. They are often simplified and are programmed to fit a situation as the person establishing the model sees it. This procedure can be less than perfect as can be pointed out by experimental results. On the other hand, it serves as a good guideline and usually can be handled, revised, and adjusted more easily than a laboratory set up. Models have been used extensively in the investigation of cam actuated systems. Most of the work has been done by the classical method of mechanics, i.e., a free body diagram with force analysis, [1], [2], [9], [18], [19], [7], [20]. The technique used is to set up the free body diagram

and solve the resulting differential equations. Graphical application to solve for acceleration, velocity and displacement polygons can also be used [21].

The above references usually employ a mechanism that behaves properly, i.e., the cam and pushrod stay in contact and problems such as pushrod bounce, valve bounce, impact loads, cam machine surface errors are not considered, or are considered alone and not in connection with each other. Barkan and McGarrity [20] did consider impact loads on takeup of initial cam clearances, and R. C. Johnson [22] studied the impact force in a system using finite mass and infinite mass assumptions. First he calculated the forces between two bodies of finite mass. Next he assumed one of the bodies, the driving element, to have an infinite mass and calculated the force for this case. In this way he obtained a range of expected impact force values. Rothbart [7] in Chapter 8 and Neklutin [23], [15] provide insight into the problem to be expected with vibrations internal to a mechanism. Mitchell [5] also considered the interaction of cam profiles with the resonance set up at the natural frequencies of the mechanism. Rothbart, Chapter 10 [7] gives expected dynamic results of cam surface machining error and the response to the system.

One of the best and most comprehensive studies of valve train dynamic response is that of Barkan [19]. He established a valve train mechanism which he compared to experimental results. His model was developed by the technique of lumped parameters. The lumped masses were connected by massless springs of rigidity determined by the particular components. Included in the mechanism was internal and external viscous damping. Forces caused by internal combustion and by the valve spring were externally applied to the mechanism.

Differential equations used in solution of Barkan's mechanism were solved by an integration technique using successive time increment evaluations. This type of solution technique is also demonstrated in Rothbart [15] page 240, and Timoshenko and Young [24].

R. C. Winfrey [25] adapted matrix algebra to the solution of the equation of motion developed in mechanism analysis. This, coupled with the calculation ability and speed of a digital computer, reduces the amount of labor involved in the arithmetic to a much more elementary level. The technique for obtaining the equations is that developed in Rubinstein's text [26].

Applying the tool, matrix algebra, to the model which will be described later gives the potential of studying many features of a mechanism response when subjected to various operating situations. The attempt is to produce a simplified, adaptable model which can examine not only the ideal situations, but also the response to abnormal or undesirable circumstances.

This thesis deals with situations which should not occur on normal valve train systems. This is done to impress the reader with the capabilities of the model. Examined will be impact loads, valve bounce, pushrod bounce, excessive cam speed, machining errors, and cam profile. The model is capable of giving a voluminous amount of data to pinpoint response analysis. It is adaptable to various types of mechanism analysis and lends itself well to the possibility of being incorporated on a computer graphics display.

II. THEORETICAL MODEL AND APPLICATION
OF EQUATIONS OF MOTION

The model shown in Figure 1 is a simplified adaptation of the valve train system of an automobile engine. It consists of a cam, pushrod or cam follower, rocker arm, valve stem, valve spring, and valve seat. The rocker arm pivots on the rocker. It is pinned to the pushrod at one end and to the valve stem at the other end, thereby restricting all members to remain in contact. The valve spring is assumed to have a spring constant of 245 pounds per inch, is connected at the pin to the rocker arm and valve stem at one end and is fixed to ground at the other end.
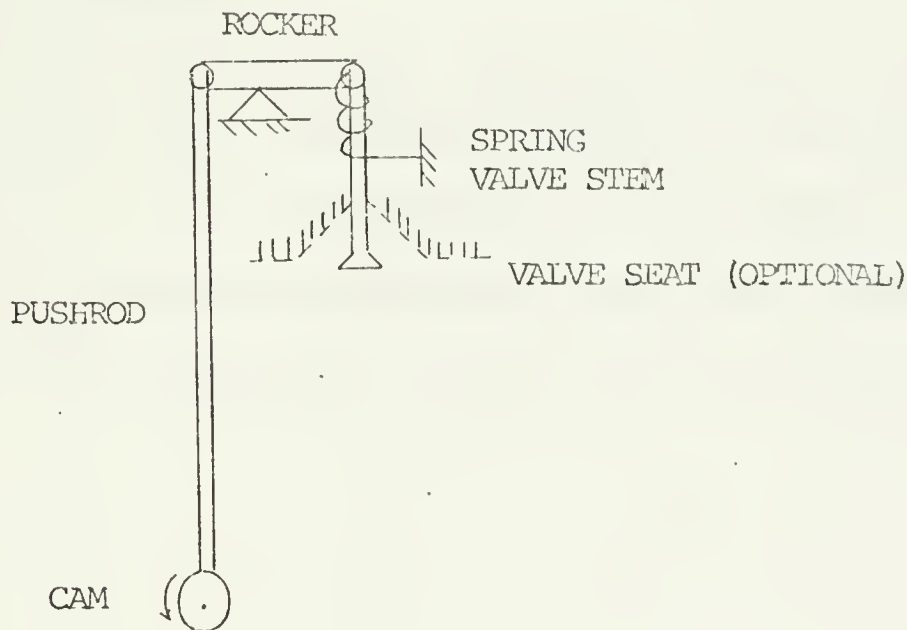

FIGURE 1. BASIC MODEL

12

The mechanism is acted on at one end by the cam in contact with the pushrod or cam follower. On the other end the valve may be acted on by the valve seat. The model is further simplified by each member having a constant circular cross section.

The valve seat position is adjustable, dependent upon the desired output. It is identified by a dashed line in Figure 1 signifying that it is not always simulated in the system. For some applications the valve is allowed to move freely, unimpeded by the valve seat.

A. EQUATIONS OF MOTION

The equations of motion,

$$[M]\{\ddot{q}\} + [C]\{\dot{q}\} + [K]\{q\} = \{F\} \tag{1}$$

were adapted to the model. The coefficients of the mass, stiffness and damping matrices were determined by the finite element technique [26].

1. System Coordinates

The system coordinates were established as shown in Figure 2. It was assumed that these coordinates accounted for all relevant energy. A linear model (i.e., small deformations) was also assumed. In this way tension and compression forces were all that were considered in the pushrod, valve stem, and spring, and only the bending forces in the rocker arm.

13
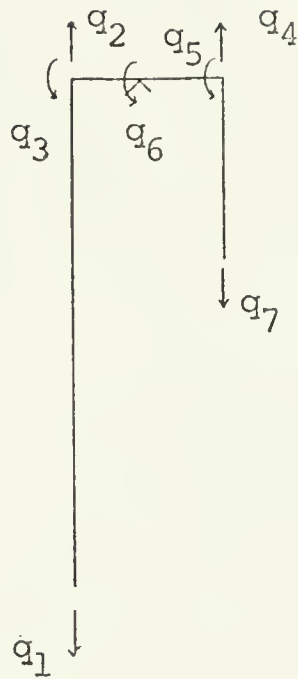
FIGURE 2. SYSTEM COORDINATES

2. Element Coordinates

Figure 3 gives the element breakdown of the system with the corresponding element coordinates. Again it is noted that elements 1, 4 and 5 (i.e., the pushrod, spring, and valve stem) are treated as axial members and elements 2 and 3 (i.e., the rocker arm) are treated as bending members. The rocker arm was divided into two elements to better represent the bending motion at the pivot.

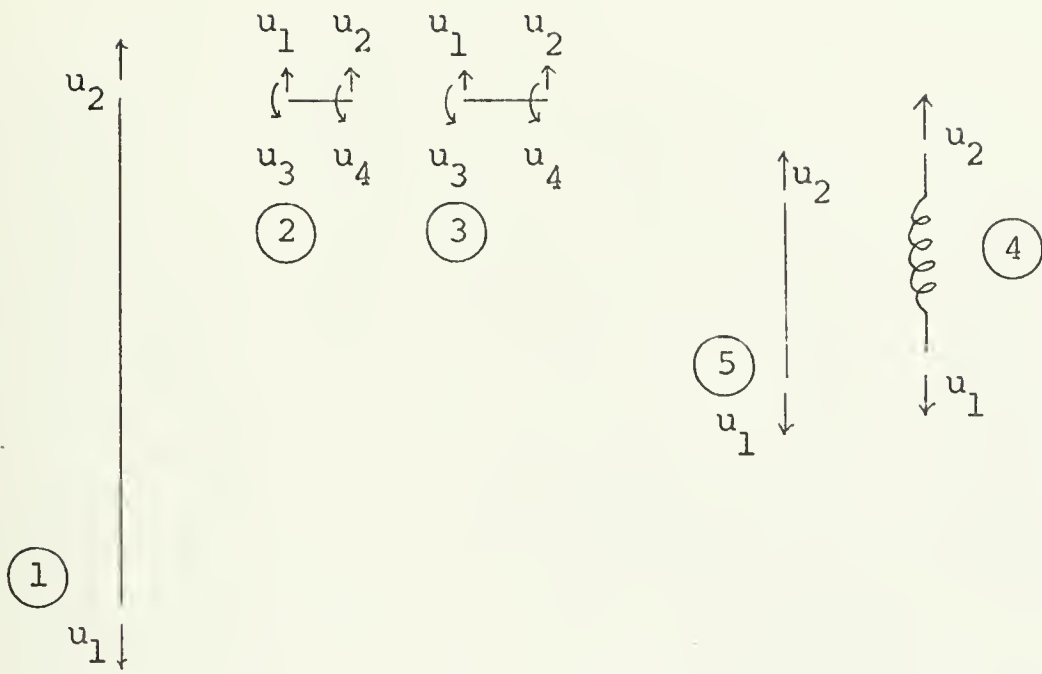FIGURE 3. ELEMENT COORDINATES

3. System Mass and Stiffness Matrices

The system coordinates, $\{q\}$, are related to the element

coordinates, $\{u\}$ by a transformation matrix $[\beta]$ as shown in Equation 2.

$$\{u\} = [\beta]\{q\} \qquad\qquad (2)$$

$[\beta]$ is formed by applying the condition of compatibility to the mechanism,

and it is evaluated in Equation 3 for the model of Figures 2 and 3.

$$
\begin{Bmatrix}
\begin{Bmatrix} u_1 \\ u_2 \end{Bmatrix}_1 \\[4pt]
\begin{Bmatrix} u_1 \\ u_2 \\ u_3 \\ u_4 \end{Bmatrix}_2 \\[4pt]
\begin{Bmatrix} u_1 \\ u_2 \\ u_3 \\ u_4 \end{Bmatrix}_3 \\[4pt]
\begin{Bmatrix} u_1 \\ u_2 \end{Bmatrix}_4 \\[4pt]
\begin{Bmatrix} u_1 \\ u_2 \end{Bmatrix}_5
\end{Bmatrix}
=
\begin{bmatrix}
1 & 0 & 0 & 0 & 0 & 0 & 0 \\
0 & 1 & 0 & 0 & 0 & 0 & 0 \\
\hline
0 & 1 & 0 & 0 & 0 & 0 & 0 \\
0 & 0 & 0 & 0 & 0 & 0 & 0 \\
0 & 0 & 1 & 0 & 0 & 0 & 0 \\
0 & 0 & 0 & 0 & 0 & 1 & 0 \\
\hline
0 & 0 & 0 & 0 & 0 & 0 & 0 \\
0 & 0 & 0 & 1 & 0 & 0 & 0 \\
0 & 0 & 0 & 0 & 0 & 1 & 0 \\
0 & 0 & 0 & 0 & 1 & 0 & 0 \\
\hline
0 & 0 & 0 & 0 & 0 & 0 & 0 \\
0 & 0 & 0 & 1 & 0 & 0 & 0 \\
\hline
0 & 0 & 0 & 0 & 0 & 0 & 1 \\
0 & 0 & 0 & 1 & 0 & 0 & 0
\end{bmatrix}
\begin{Bmatrix}
q_1 \\ q_2 \\ q_3 \\ q_4 \\ q_5 \\ q_6 \\ q_7
\end{Bmatrix}
\qquad (3)
$$

As noted in Equation 3, $[\beta]$ is partitioned into sub-matrices according to elements. Equation 3 may thus be rewritten in a more concise form,

$$
\begin{Bmatrix}
\{u\}_1 \\ \{u\}_2 \\ \{u\}_3 \\ \{u\}_4 \\ \{u\}_5
\end{Bmatrix}
=
\begin{Bmatrix}
[\beta]_1 \\ [\beta]_2 \\ [\beta]_3 \\ [\beta]_4 \\ [\beta]_5
\end{Bmatrix}
\{q\} .
\qquad (4)
$$

Utilizing the transformation matrix $[\beta]$ and the procedure of Chapter 7 of reference [26] the system mass and stiffness matrices, $[M]$ and $[K]$, were formed.

As shown in the reference, $[\beta]$ relates the stiffness and mass properties of the elements to the stiffness and mass properties of the system.

$$[K] = \sum_{i=1}^{5} [\beta]_i^T [K_e]_i [\beta]_i \qquad (5)$$

$$[M] = \sum_{i=1}^{5} [\beta]_i^T [M_e]_i [\beta]_i \qquad (6)$$

$[\beta]_i$ is the submatrix of $[\beta]$ corresponding to the i^{TH} element. Similarly, $[K_e]_i$ and $[M_e]_i$ are the i^{TH} element stiffness and mass matrices. The element stiffness matrices are given by [25].

$$[K_e]_i = \frac{E_i A_i}{L_i} \begin{bmatrix} 1 & 1 \\ 1 & 1 \end{bmatrix} \qquad (i = 1,4,5) \qquad (7)$$

and

$$[K_e]_i = \frac{E_i I_i}{L_i^3} \begin{bmatrix} 12 & -12 & 6L_i & 6L_i \\ -12 & 12 & -6L_i & -6L_i \\ 6L_i & -6L_i & 4L_i^2 & 2L_i^2 \\ 6L_i & -6L_i & 2L_i^2 & 4L_i^2 \end{bmatrix} \qquad (8)$$
$$(i = 2,3)$$

and the element mass matrices are:

$$[M_e]_i = \frac{M_i}{6} \begin{bmatrix} 2 & -1 \\ -1 & 2 \end{bmatrix} \qquad (i = 1,4,5) \qquad (9)$$

And,

$$[M_e]_i = \frac{M_i}{420} \begin{bmatrix} 156 & 54 & 22L_i & -13L_i \\ 54 & 156 & 13L_i & -22L_i \\ 22L_i & 13L_i & 4L_i^2 & -3L_i^2 \\ -13L_i & -22L_i & -3L_i^2 & 4L_i^2 \end{bmatrix} \quad (i = 2,3) \quad (10)$$

In the above equations, E_i is the elastic modulus, A_i is the cross sectional area, L_i is the length, and M_i is the total mass of the i^{TH} element.

    a. Stiffness Matrix

        Evaluating Equation 5 for [K] gives Equation 11 (see page 19).

    b. Mass Matrix

        Matrix multiplication of Equation 6 yields for the system mass matrix, Equation 12 (see page 20).

    4. <u>System Damping Matrix</u>

        The system damping matrix is formed in two steps. First, the equation of motion without damping is uncoupled and is written in terms of modal coordinates. Next, by the use of the diagonal matrices of the normalized equation of motion, the damping matrix can be developed.

    a. Equation of Motion in Terms of Modal Coordinates

        Rewriting the equation of motion, Equation 1, without damping yields:

$$[M]\{\ddot{q}\} + [K]\{q\} = \{F\}. \quad (13)$$

$$[K] = \begin{bmatrix}
\dfrac{E_1 A_1}{L_1} & \dfrac{E_1 A_1}{L_1} & 0 & 0 & 0 & 0 & 0 \\[4mm]
\dfrac{E_1 A_1}{L_1} & \dfrac{E_1 A_1}{L_1} + \dfrac{12 E_2 I_2}{L_2^{3}} & \dfrac{6 E_2 I_2}{L_2^{2}} & 0 & 0 & \dfrac{6 E_2 I_2}{L_2^{2}} & 0 \\[4mm]
0 & \dfrac{6 E_2 I_2}{L_2^{2}} & \dfrac{4 E_2 I_2}{L_2} & 0 & 0 & \dfrac{2 E_2 I_2}{L_2} & 0 \\[4mm]
0 & 0 & 0 & \dfrac{12 E_3 I_3}{L_3^{3}} + \dfrac{E_5 A_5}{L_5} + \dfrac{E_4 A_4}{L_4} & \dfrac{-6 E_3 I_3}{L_3^{2}} & \dfrac{-6 E_3 I_3}{L_3^{2}} & \dfrac{E_5 A_5}{L_5} \\[4mm]
0 & 0 & 0 & \dfrac{-6 E_3 I_3}{L_3^{2}} & \dfrac{4 E_3 I_3}{L_3} & \dfrac{2 E_3 I_3}{L_3} & 0 \\[4mm]
0 & \dfrac{6 E_2 I_2}{L_2^{2}} & \dfrac{2 E_2 I_2}{L_2} & \dfrac{-6 E_3 I_3}{L_3^{2}} & \dfrac{2 E_3 I_3}{L_3} & \dfrac{4 E_3 I_3}{L_3} + \dfrac{4 E_2 I_2}{L_2} & 0 \\[4mm]
0 & 0 & 0 & \dfrac{E_5 A_5}{L_5} & 0 & 0 & \dfrac{E_5 A_5}{L_5}
\end{bmatrix} \tag{11}$$

$$[M] =
\begin{bmatrix}
\dfrac{M_1}{3} & \dfrac{-M_1}{6} & 0 & 0 & 0 & 0 & 0 \\[2em]
\dfrac{-M_1}{6} & \dfrac{M_1}{3}+\dfrac{156M_2}{420} & \dfrac{22M_2L_2}{420} & 0 & 0 & \dfrac{-13L_2M_2}{420} & 0 \\[2em]
0 & \dfrac{22L_2M_2}{420} & \dfrac{4L_2M_2}{420} & 0 & 0 & \dfrac{-3L_2^2M_2}{420} & 0 \\[2em]
0 & 0 & 0 & \dfrac{156M_3}{420}+\dfrac{M_4}{3}+\dfrac{M_5}{3} & \dfrac{-22L_3M_3}{420} & \dfrac{13L_3M_3}{420} & \dfrac{-M_5}{6} \\[2em]
0 & 0 & 0 & \dfrac{-22L_3M_3}{420} & \dfrac{4L_3^2M_3}{420} & \dfrac{-3L_3^2M_3}{420} & 0 \\[2em]
0 & \dfrac{-13L_2M_2}{420} & \dfrac{-3L_2^2M_2}{420} & \dfrac{13L_3M_3}{420} & \dfrac{-3L_3^2M_3}{420} & \dfrac{4L_2^2M_2}{420} & 0 \\[2em]
0 & 0 & 0 & \dfrac{-M_5}{6} & 0 & 0 & \dfrac{M_5}{3}
\end{bmatrix}$$

(12)

Having the mass and stiffness matrices, the eigenvalue
problem may be solved using Equation 14.

$$(\omega^2 [M] - [K])\{q\} = \{0\} \qquad (14)$$

This gives a solution of seven eigenvalues, ω_i $(i = 1,2,...7)$, and seven
corresponding eigenvectors or mode shapes, $\{\phi\}_i$. Arranging the
eigenvectors in columns,

$$[\phi] = [\{\phi\}_1 \ \{\phi\}_2 \ \{\phi\}_3 \ \{\phi\}_4 \ \{\phi\}_5 \ \{\phi\}_6 \ \{\phi\}_7] \qquad (15)$$

gives the modal matrix, $[\phi]$, which may be used as a coordinate transfor-
mation matrix to uncouple Equation 13. This gives the equation of motion
in terms of the modal coordinates,

$$[M]\{\ddot{\eta}\} + [K]\{\eta\} = \{F_n\}, \qquad (16)$$

where $\{F_n\}$ is the modal force vector, and $[M]$ and $[K]$ are the diagonal,
or uncoupled, mass and stiffness matrices related to $[M]$ and $[K]$ by,

$$[M] = [\phi]^T [M] [\phi] \qquad (17)$$

$$[K] = [\phi]^T [K] [\phi] \qquad \cdot \qquad \cdot \qquad (18)$$

$\{\ddot{\eta}\}$ and $\{\eta\}$ are a set of system modal coordinates related
to the system coordinates $\{\ddot{q}\}$ and $\{q\}$ by,

$$\{\ddot{q}\} = [\phi]\{\ddot{\eta}\} \qquad (19)$$

$$\{q\} = [\phi]\{\eta\} \qquad (20)$$

b. Formation of [C]

Having $[M]$ and $[K]$, $[C]$ can be formed and $[C]$ solved for by
matrix manipulation and multiplication.

The eigenvalues, ω_i, equal $\sqrt{\dfrac{k_{ii}}{m_{ii}}}$ with k_{ii} and m_{ii} equal
to the diagonal elements of $[K]$ and $[M]$, respectively. The modal system
is assumed to have viscous damping, so that the values on the diagonal
of $[C]$, c_{ii}, are related to k_{ii} and m_{ii} by,

$$c_{ii} = 2\zeta_i \sqrt{k_{ii}m_{ii}} , \qquad (i = 1,2,\ldots 7) \qquad (21)$$

where ζ_i is the damping ratio. The damping ratio, ζ, of the fundamental
mode was set equal to 0.5 and the other six modes of higher frequency
were set equal to 0.1.

The system damping matrix $[C]$ can now be found from $[C]$ as
follows:

$$[C] = [\phi]^T [C] [\phi] \qquad (22)$$

Thus,

$$[C] = [\phi^T]^{-1} [C] [\phi]^{-1} \qquad (23)$$

22

III. ADAPTATION OF MODEL TO PROBLEM SOLUTION

The model established in Figure 1 and the equation of motion established in Section II can now be used to examine dynamic reactions of the model to applied situations.

There are two coordinates of the model acted upon by external forces: coordinate one and coordinate seven. Coordinate one is the displacement of the point on the pushrod which comes in contact with the cam, and coordinate seven is the displacement of the point on the valve which comes in contact with the valve seat. Depending on the value of the force and displacement at these two coordinates, the model can exist as one of four possible configurations; (1) contact between the cam and pushrod and no contact between the valve and valve seat; (2) no external contact at cam or valve seat; (3) contact between cam and pushrod and valve and valve seat; and (4) contact between valve and valve seat and no contact between cam and pushrod. These four configurations will be referred to as configurations I through IV, and will be described in more detail shortly.

The model will fall into one of the above configurations at all times, but will remain in any configuration only as long as the physical constraints of the model are satisfied. Certain coordinate values, listed in Table I, are monitored to indicate when the model shifts from one configuration to another. As an example, at coordinate one the force, F_1, between the cam and pushrod must have a negative value. The negative value is due to the choice of the direction of coordinate one and the fact that the cam can only push on the pushrod and cannot pull. Therefore, in the solution of F_1, if the value changes from a negative to a positive value the mechanism is no longer acting within its constraints and the model

TABLE I
CONFIGURATION RELATIONSHIP

CONFIGURATIONS	CONTACT COORDINATED	KNOWNS	MONITORED VALUES
I	1 (Pushrod)	$q_1, \dot{q}_1, \ddot{q}_1 = $ Cam Profile $F_i = 0 \quad i = 2,3,\ldots 7$	F_1, q_7
II	None	$F_i = 0 \quad i = 1,2,\ldots 7$	q_1, q_7
III	1,7 (Pushrod and Valve)	$q_1, \dot{q}_1, \ddot{q}_1 = $ Cam Profile $q_7 = $ Valve Seat Position $\dot{q}_7, \ddot{q}_7 = 0$ $F_i = 0 \quad i = 2,3,\ldots 6$	F_1, F_7
IV	7 (Valve)	$q_7 = $ Valve Seat Position $\dot{q}_7, \ddot{q}_7 = 0$ $F_i = 0 \quad i = 1,2,\ldots 6$	q_1, F_7

must shift to another configuration, in this case configuration II, which allows for no external forces. The value of F_1 will remain equal to zero until the pushrod comes back in contact with the cam.

The equations of motion for the four configurations differ slightly from one another. The rearrangement of the basic equation of motion, Equation 1, for each configuration is such as to take advantage of the known values of coordinate displacement, velocity, acceleration, and force for that particular configuration. The known values for each configuration are given in Table I. The adaption of the equation of motion, Equation 1, to each configuration and the solution technique are given in Appendix A. As can be seen in Appendix A, each configuration has a set of equations having the same form as Equation 1. This solution is done by the integration procedure described in Appendix B. An explanation of each configuration follows.

A. CONFIGURATION I

This is the basic configuration. In this configuration, contact is between pushrod and cam only. Each of the examples studied later begins in this configuration. The force at coordinate one and the displacement at coordinate seven, are monitored to determine when the model is to shift into configuration II or III.

1. Force at Coordinate One

Due to the selection of the direction of coordinate one, the force must be negative for any contact. A positive value for F_1, indicates a shift to configuration II, free of external forces. The value of the force at F_1 is obtained from the first row of Equation 1.

$$F_1 = \sum_{i=1}^{7} (m_{1i}\ddot{q}_i + c_{1i}\dot{q}_i + k_{1i}q_i) \qquad (26)$$

25

2. Displacement at Coordinate Seven

The value of q_7 is monitored in those problems in which a valve seat is considered. The valve seat is simulated as having a particular position and when interference between the valve and valve seat occurs the model shifts to configuration III, contact at both the cam and valve seat.

B. CONFIGURATION II

In this section the model is in the free or "floating" state. There are no external forces on the model and it moves freely based on its natural frequencies and its initial conditions when it assumed this configuration. The valve spring acts on the system as an internal member to bring the system back in contact with the valve seat or cam. The monitoring of q_1 and q_7 indicates which contact happens first.

1. Displacement at Coordinate One

q_1 is monitored against the position of the cam. When interference occurs between the cam and pushrod, the model shifts into configuration I, contact between cam and pushrod.

2. Displacement at Coordinate Seven

q_7 is monitored against the position of the valve seat and when it exceeds the valve seat position the model shifts to configuration IV, contact between valve and valve seat.

C. CONFIGURATION III

In configuration III, both the cam and valve seat are in contact. This configuration may be thought of as a cross-over configuration. The model will not remain in this configuration as long as it does in the

26

other three configurations. The model enters configuration III from configuration I or IV. In configuration I, the model has been in contact with the cam and in configuration IV, the model has been in contact with the valve seat.

Since the model is elastic, it will shortly lose contact at one of the two contact points. Viewing Figure 1 it can be seen that when the valve is in contact with its seat, and the cam comes in contact with the pushrod, the end result will be to quickly push the valve away from the seat, and hence transfer to configuration I. When the pushrod is running on the cam and the valve comes in contact with the seat, the end result will be to lift the pushrod away from the cam and transfer to configuration IV.

The two external force values, F_1 and F_7 are monitored.

1. Force at Coordinate One

The force at coordinate one is monitored in the same manner as configuration I. When F_1 shifts from a negative to a positive value, the pushrod loses contact with the cam and the model shifts to con configuration IV.

2. Force at Coordinate Seven

The force at coordinate seven is monitored by solving the last row of Equation 1.
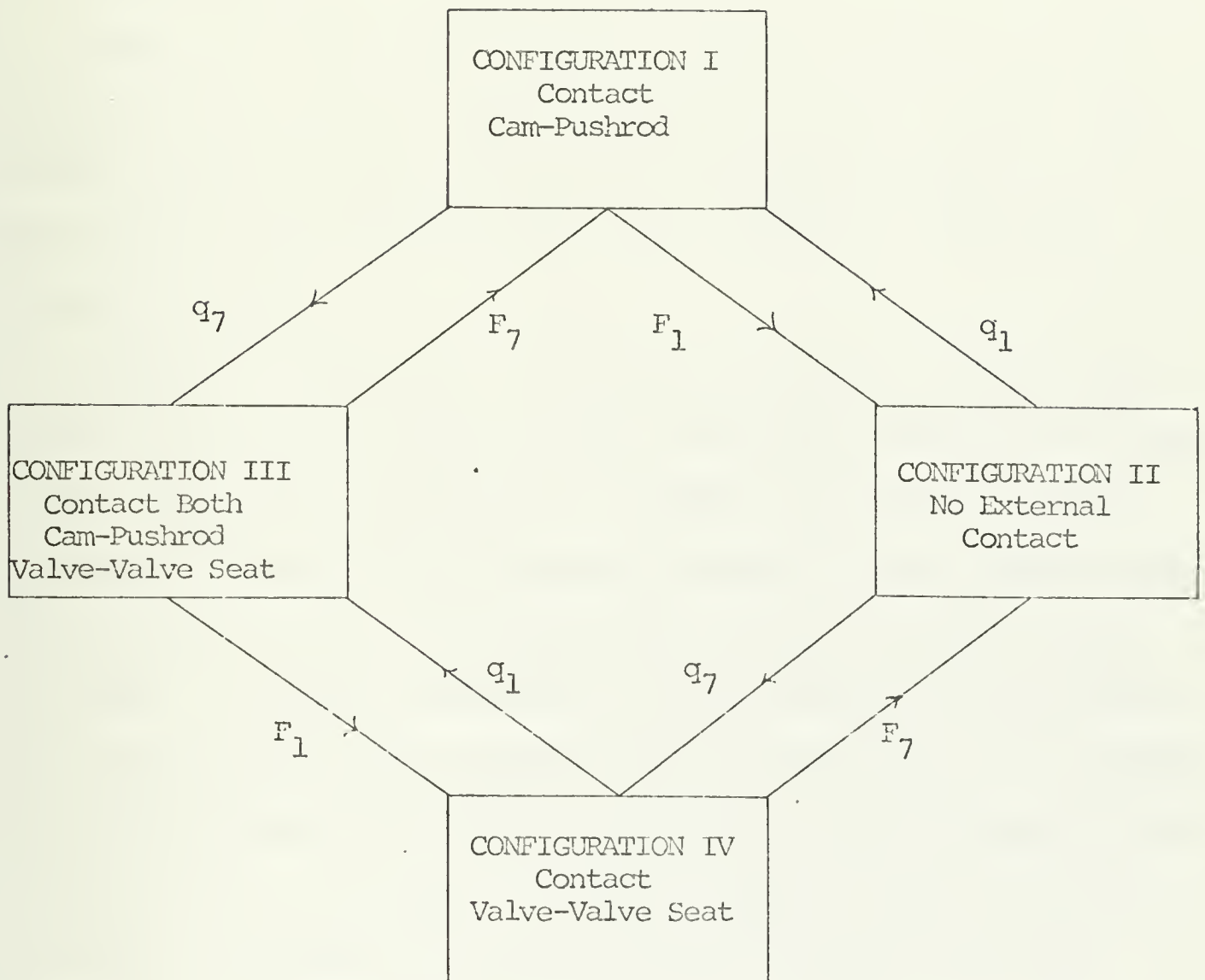
$$F_7 = \sum_{i=1}^{7} (m_{7i}\ddot{q}_i + c_{7i}\dot{q}_i + k_{7i}q_i) \qquad (27)$$

Due to the selection of the direction of coordinate seven, when the value of F_7 changes from positive to negative, contact at coordinate seven has been lost and the model shifts to configuration I.

27

D. CONFIGURATION IV

Configuration IV indicates contact at the valve and valve seat only. The values q_1 and F_7 are monitored in the same manner as previously described and indicate when the model shifts to configuration III or II respectively.

Figure 4 gives a schematic of the four configurations, their relationship to each other, and the coordinate values monitored between any two configurations.

CONFIGURATION I
Contact
Cam-Pushrod

CONFIGURATION III
Contact Both
Cam-Pushrod
Valve-Valve Seat

CONFIGURATION II
No External
Contact

CONFIGURATION IV
Contact
Valve-Valve Seat

q_7 F_7 F_1 q_1

q_1 q_7 F_1 F_7

Values on diagonal lines are monitored to determine when to shift to another configuration. Arrow indicates direction of shift.

FIGURE 4.   INTERRELATIONSHIP OF CONFIGURATIONS

IV.   IMPACT FORCE ANALYSIS

A.   BACKGROUND

Impact in the model occurs when the cam and pushrod or valve and valve seat came together.   Impact forces are difficult to predict accurately and most often are studied from an elemental standpoint, i.e., two idealized masses impacting with smooth surfaces and relatively simplified geometry.

Background investigation to determine the manner of handling impact forces in model analysis does not yield much useful information for this thesis.   The cam was assumed to be an infinite mass with its velocity unchanged by impact.   As was explained in Chapter I, this assumption was one of the two used by R. C. Johnson [22] to predict a range of values for impact.   Timoshenko and Goodier [27] also studied colliding members. The above references dealt basically with two masses and did not consider an elastic mechanism with interacting members.   Of prime interest was the local deformation and stresses produced at point of impact, whereas in this thesis, deformation of the entire system is taken into account rather than local deformation.

Barkan and McGarrity [20] mention impact forces in a valve train system, but only from the standpoint of the takeup of initial clearance between cam and pushrod.   Once their system began to operate there was no later separation.

Dubowsky and Freudenstein, [28], [29], also deal with the problem of clearances in mechanical systems.   They developed a dynamic model for their study and examined the system response.   Their study deals with clearances at pins and points of connection and does not deal with the effect of large impact forces on a system.

30

Thoren, Engemann, and Stoddart [3] did consider valve bounce as
related to the design of cam contours. They conducted laboratory studies
of different types of valve trains and with different cam profiles. They
did not set up an analytical model for a valve train, and did not consider
the effects of such situations as pushrod and cam separation and impact.
In addition, they were mainly interested in valve displacements and did
not measure contact forces.

B. MODEL IMPACT FORCE CALCULATIONS

The integration technique of Appendix B used in the solution of the
equation of motion finds displacement, velocity, and acceleration over
successive time steps, ΔT. Figures 5, 6, and 7 give idealized curves of
$\dot{q}$ and $\ddot{q}$ for a particular coordinate which undergoes a sharp change in
its displacement profile, q. This produces a step input to the velocity
curve and an impulse to the acceleration profile. Figures 8, 9, and 10
are the modifications to the idealized case which are necessary to
account for the modeling limitation of Appendix B. Changes can only
occur during an integration interval, ΔT.

Figure 8 is identical to Figure 5. Differentiation of the displace-
ment yields Figure 9 for the velocity curve. As shown it takes one time
step to reach the step input value in Figure 6. Differentiation to
obtain acceleration yields Figure 10. It takes two time intervals to
account for the impulse in Figure 7 and reduce the acceleration curve
again to zero. The value of acceleration at time t_2 is given by the
equation,

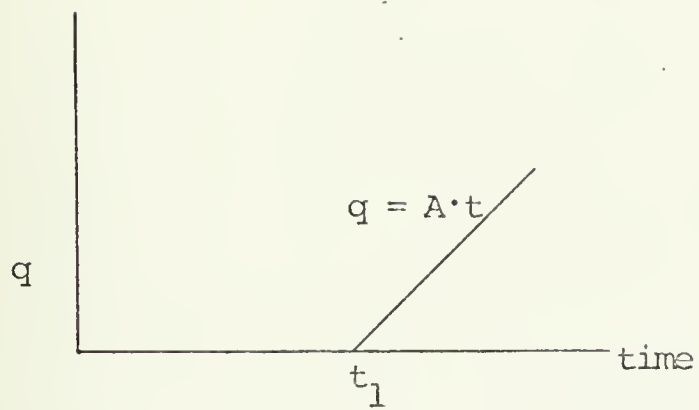$$\ddot{q}_{t_2} = \dot{q}_{t_2}/\Delta T. \qquad (28)$$
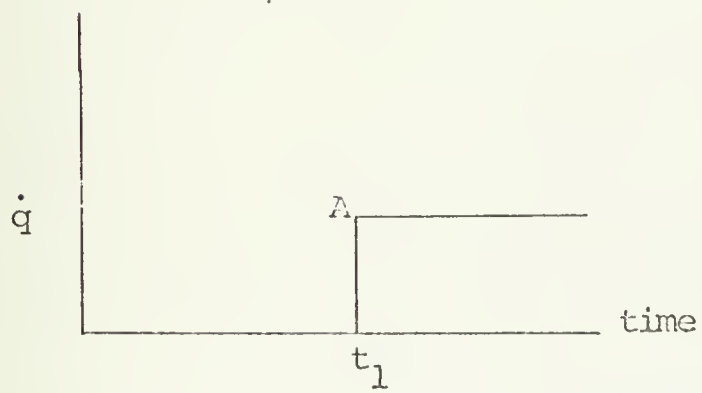
31

FIGURE 5.   Ideal Displacement Curve
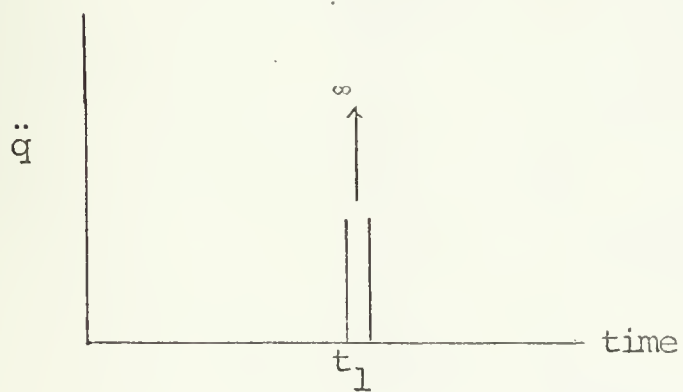

FIGURE 6.   Ideal Velocity Curve

FIGURE 7.   Ideal Acceleration Curve

32

$$q = A \cdot t$$

q

t_1
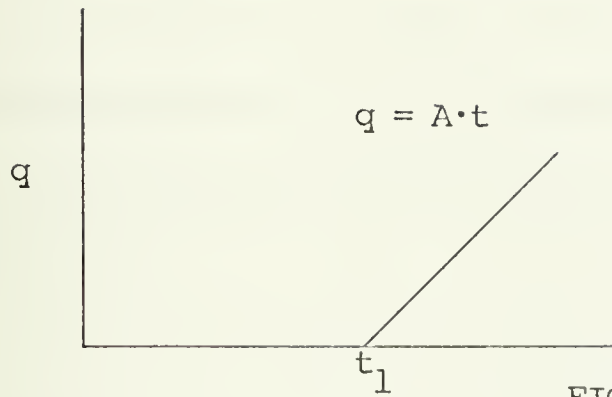
FIGURE 8. Model Displacement Curve

$\dot{q}$

$$\dot{q}_{t_2} = A$$

$$\Delta T = t_2 - t_1$$

$t_1 t_2$

FIGURE 9. Model Velocity Curve

$\ddot{q}$

$$\ddot{q}_{t_2} = A/\Delta T$$

$$\Delta T = t_3 - t_2 = t_2 - t_1$$

$t_1 t_2 t_3$
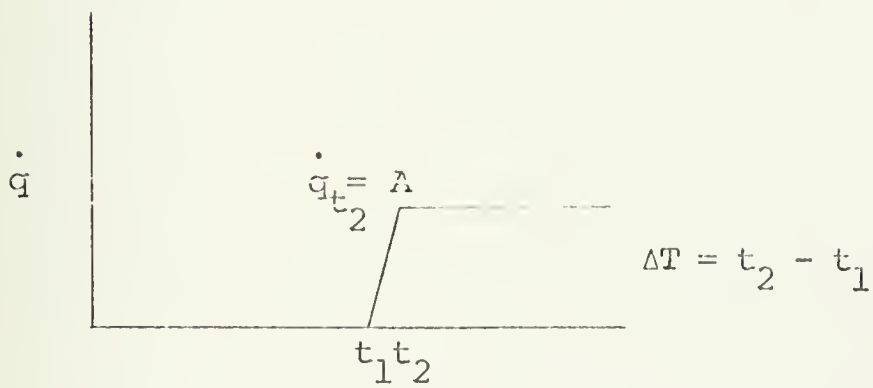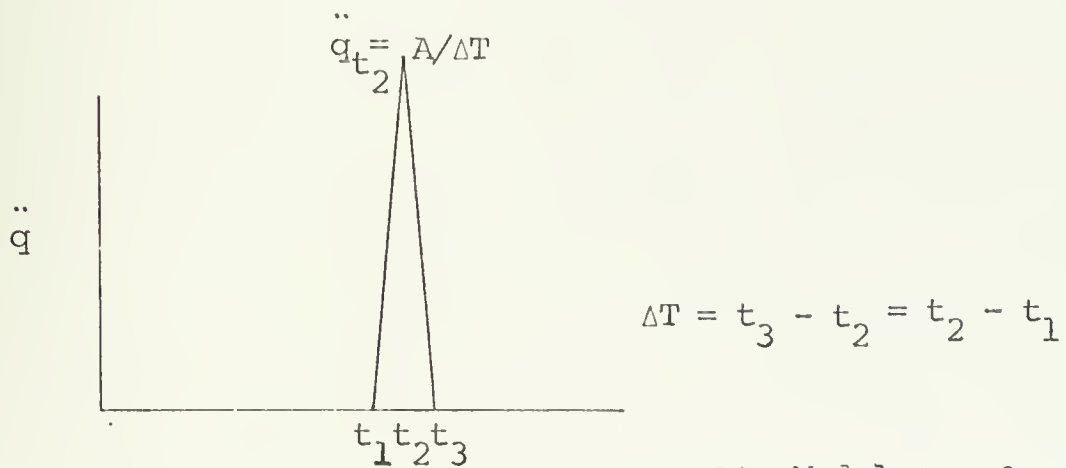
FIGURE 10. Model Acceleration Curve

Note also, that due to the value of $\ddot{q}_{t_2}$, which will usually be fairly high since ΔT is small, the value of F_{t_2}, the force at the coordinate in question, can be significantly higher than F_{t_1} or F_{t_3}. This is to be expected at the instant of impact.

V. RESULTS

Figures 11 and 12 are the numerical values of the [M] and [K] matrices respectively. These were obtained by first substituting the values of Table II into Equations 11 and 12 to get the mass and stiffness matrices [M] and [K].

MASS MATRIX [M]

$$
\begin{bmatrix}
15.5 & -7.8 & 0.0 & 0.0 & 0.0 & 0.0 & 0.0 \\
-7.8 & 23.2 & 1.1 & 0.0 & 0.0 & -.6 & 0.0 \\
0.0 & 1.1 & .2 & 00.0 & 0.0 & -.1 & 0.0 \\
0.0 & 00.0 & 0.0 & 20.1 & -2.4 & 1.4 & -2.6 \\
0.0 & 0.0 & 0.0 & -2.4 & .6 & -.5 & 0.0 \\
0.0 & -.6 & -.1 & 1.4 & -.5 & .9 & 0.0 \\
0.0 & 0.0 & 0.0 & -2.6 & 0.0 & 0.0 & 5.2
\end{bmatrix} \times 10^{-5}
$$

FIGURE 11

STIFFNESS MATRIX [K]

$$
\begin{bmatrix}
2.4 & 2.4 & 0.0 & 0.0 & 0.0 & 0.0 & 0.0 \\
2.4 & 25.2 & 11.5 & 0.0 & 0.0 & 11.5 & 0.0 \\
0.0 & 11.5 & 7.6 & 0.0 & 0.0 & 3.8 & 0.0 \\
0.0 & 0.0 & 0.0 & 13.8 & -5.1 & -5.1 & 7.1 \\
0.0 & 0.0 & 0.0 & -5.1 & 5.1 & 2.5 & 0.0 \\
0.0 & 11.5 & 3.8 & -5.1 & 2.5 & 12.7 & 0.0 \\
0.0 & 0.0 & 0.0 & 7.1 & 0.0 & 0.0 & 7.1
\end{bmatrix} \times 10^{5}
$$

FIGURE 12

TABLE II

Element	Length (L) Inches	Diameter (D) Inches
1	9.0	.3
2	1.0	.6
3	1.5	.6
4	36.0	.07
5	3.	.3

FOR ALL MEMBERS

Elastic Modulus = 30×10^6 lb/inch^2

Specific Weight = .283 lb/inch^3

With the mass and stiffness matrices formed, the eigenvalue problem

was solved and the damping matrix [C] obtained, Figure 13.

DAMPING MATRIX [C]

92.3	37.7	3.7	21.0	2.9	-4.5	6.0
37.7	217.2	33.1	67.6	-18.6	26.5	-10.7
3.7	33.1	20.2	7.2	-3.2	.1	-.5
-21.0	67.6	7.2	178.0	-37.0	-.9	83.1
2.9	-18.6	-3.2	-37.0	-27.6	-7.7	-10.0
-4.5	26.5	.1	-.9	-7.7	48.9	4.6
6.0	-10.7	-.5	83.1	10.0	4.6	95.7

$\times 10^{-2}$

FIGURE 13

Figure 14 gives the numerical values of $[\phi]$ and the values of the

seven natural frequencies, ω_i , in radians per second. $[\phi]$ is arranged

in Figure 14 so that each eigenvector $\{\phi\}_i$ is listed below its related

natural frequency ω_i.

EIGENVALUES ω_n , $\times 10^3$

25.9	1070.2	736.5	247.1	521.9	146.7	.691

EIGENVECTORS IN COLUMNS $[\phi]$

17.7	-.1	-9.4	-.5	.3	.6	-418.9
-8.1	-.2	-8.7	-.8	.6	.9	418.7
11.8	7.5	9.5	5.5	-9.6	-2.9	-418.7
-15.4	.2	-1.2	2.5	.7	2.6	-627.3
-15.4	4.4	-4.4	12.7	8.1	-3.1	-418.0
.6	4.2	5.7	-6.7	4.1	3.0	-418.5
16.6	.1	2.5	2.3	.4	8.0	627.3

$\times 10^{-4}$

FIGURE 14

In the solution of the equations of motion by the technique shown in Appendix B, the time increment, ΔT, was 1×10^{-6} second. This value was chosen so as to be approximately one fourth the period of the mode having the highest frequency. If a value of ΔT was chosen close to one of the natural periods, the solution would become unstable and quickly diverge.

Figures 15 through 32 show the results of different problems run on the model. The problems were designed to test each of the four configurations in which the model could exist. The cam profile was assumed to be harmonic with no dwells, and 1" peak to peak. There are four basic types of operating situations.

1. Contact maintained between cam and pushrod at all times without considering valve seat. In this situation the model could only exist in Configuration I.

2. Cam speed increased so that the pushrod no longer remains in contact at all times with the cam. No valve seat. In this case the model will exist in Configuration I and II.

3. Valve seat employed in the system. The cam rotated at a slow enough speed so that the pushrod would remain in contact with cam if the valve seat were not in the system. The model utilizes all four configurations.

4. A combination of 2 and 3 above. The valve seat is employed and the cam is run at a high enough speed for the pushrod to lose contact with the cam. Again all four configurations are employed in the model.

The Figures 15 through 32 are graphs of the displacement and force curves at the contact coordinates. There are two graphs for each problem in Section A and B. The first graph will show the cam profile and the

38

pushrod profile. The second graph will be the curve of F_1, the force between cam and pushrod. Included on this graph for those problems employing a valve seat will be the curve of F_7, the force between valve and valve seat. The only deviation from this will be the problem run at 20000 RPM without a valve seat. In this instance the pushrod profile was plotted on the same graph as the force profile. This was done to show the comparison of dynamic responses of force and displacement at one coordinate. For section C, Figures 33 through 41, the graphs are plotted to show the most interesting features in terms of force and/or displacement of the particular problem. It should be noted that the values plotted are done at intervals of one degree which is much larger than the integration interval, ΔT, This gives a good representation of the overall force and displacement responses with one exception - impact force values. Impact forces occur for only one integration interval, ΔT, and therefore do not always get plotted.

A. WITHOUT VALVE SEAT

  1. 9000 RPM - Figures 15 and 16

Figure 15 shows the pushrod-cam profile curve and Figure 16 the curve representing the force between the cam and pushrod. As can be seen, the value of F_1 remains negative. As has been stated previously, unless the value of F_1 changes signs from negative to positive, the pushrod-cam profile curves will be superimposed on each other.

  2. 9524 RPM - Figures 17 and 18

In Figure 18 the force reaches the zero value indicating separation of the pushrod and cam. Again it is noted that the value of F_1 can go no higher than zero for the cam cannot pull on the pushrod. Therefore, the flat part of the force profile indicates the length of time the
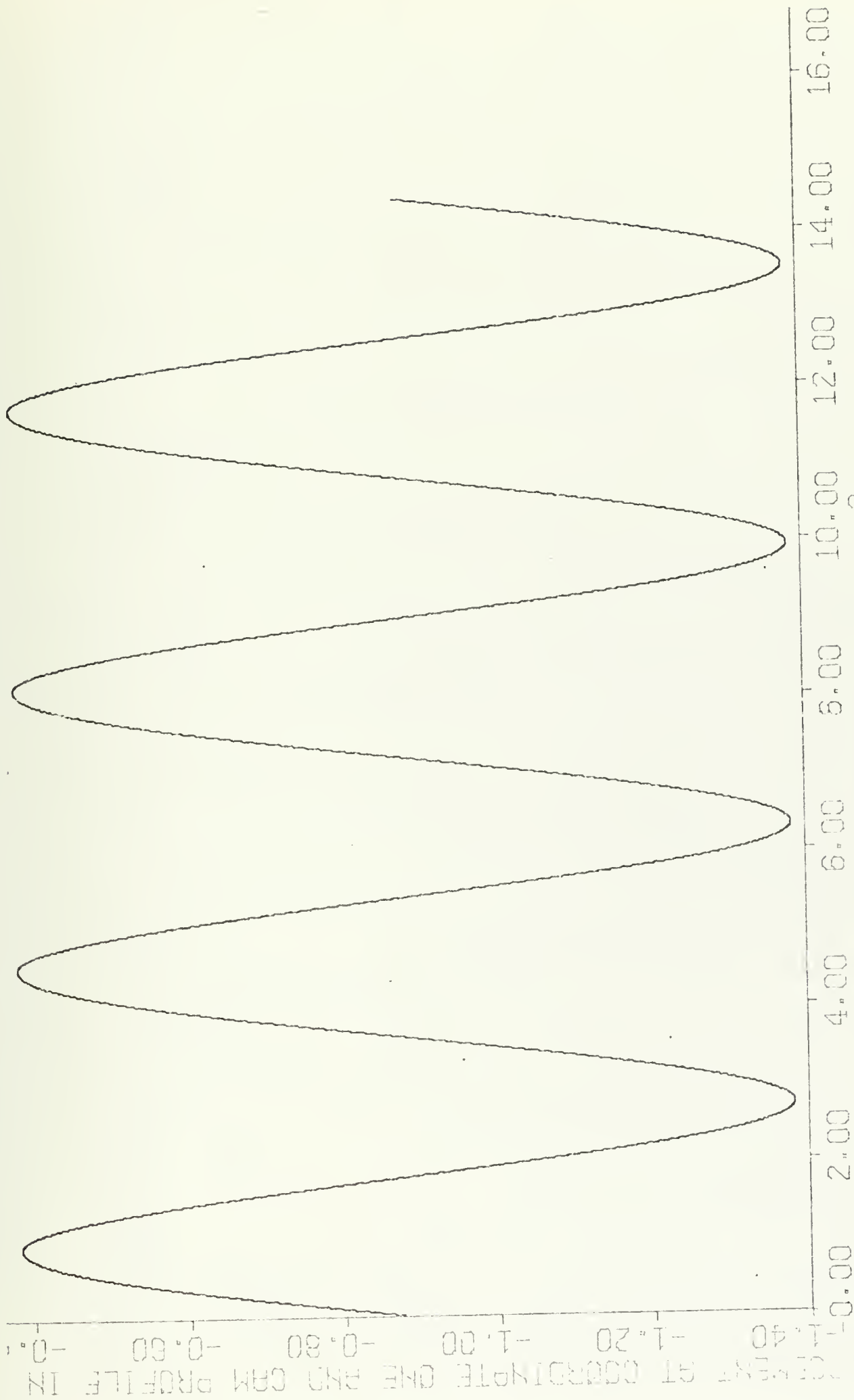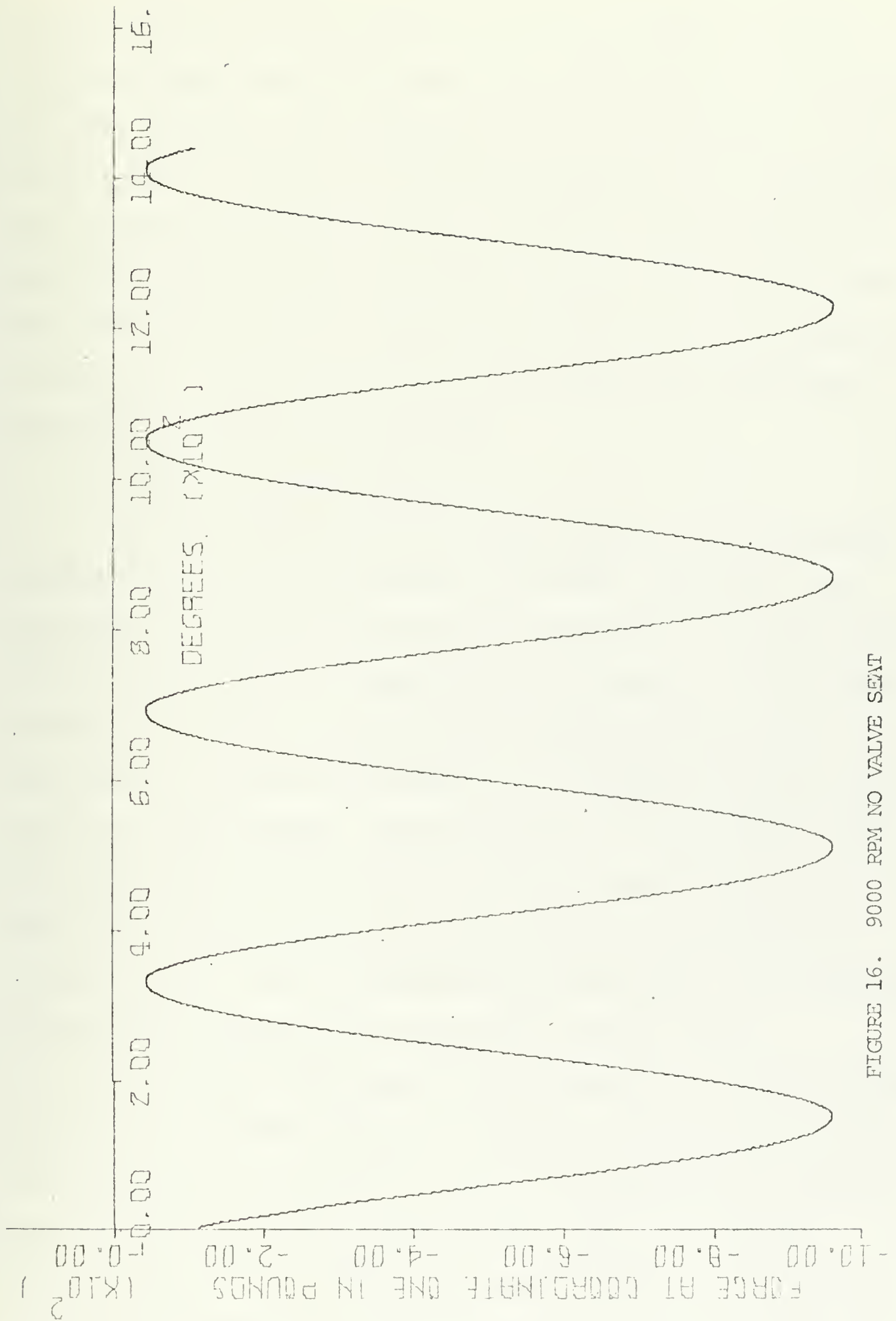
39

FIGURE 15. 9000 RPM NO VALVE SEAT

FIGURE 16. 9000 RPM NO VALVE SEAT

41

cam and pushrod are not in contact. The cam and pushrod are not in

contact for approximately 50 degrees. When the two come back in contact,

the force oscillates and is damped out by the internal damping of the

system. Figure 17 shows the cam and pushrod profiles to be superimposed,

but in actuality they should be separated for the same period of time

that the F_1 curve of Figure 18 is equal to zero. The pushrod is lifted

such a short distance from the cam surface that it is not distinguishable

in Figure 17. This separation of cam and pushrod will be shown more

effectively in Figure 19 for 11000 RPM.

3. 11000 RPM - Figures 19 and 20

To compare with 9524 RPM and show a general trend of mechanism

response the cam speed is increased to 11000 RPM. The pushrod gets

thrown from the cam for a larger fraction of the cycle, about 180 degrees,

shown on Figure 20, and is thrown further on Figure 19. It should also

be noticed that the two curves are not superimposed on each other. This

also happens in the 9524 RPM situation, but the separation was not great

enough to be distinguished. The third feature of this problem is that

upon coming back in contact with the cam, the pushrod bounces on the

cam and again loses contact for a period before it finally comes in

contact to remain. This is indicated by the separation of the pushrod-cam

profile curves and also by the flat portion of the F_1 curve.

The response of the system to ever increasing cam speed can now be

predicted. As the speed increases the pushrod will be thrown off the

cam surface and the mechanism will remain in Configuration II, free of

external forces, for longer periods of time. Also, as the speed

increases, more and more bounces of increasing magnitude take place. In

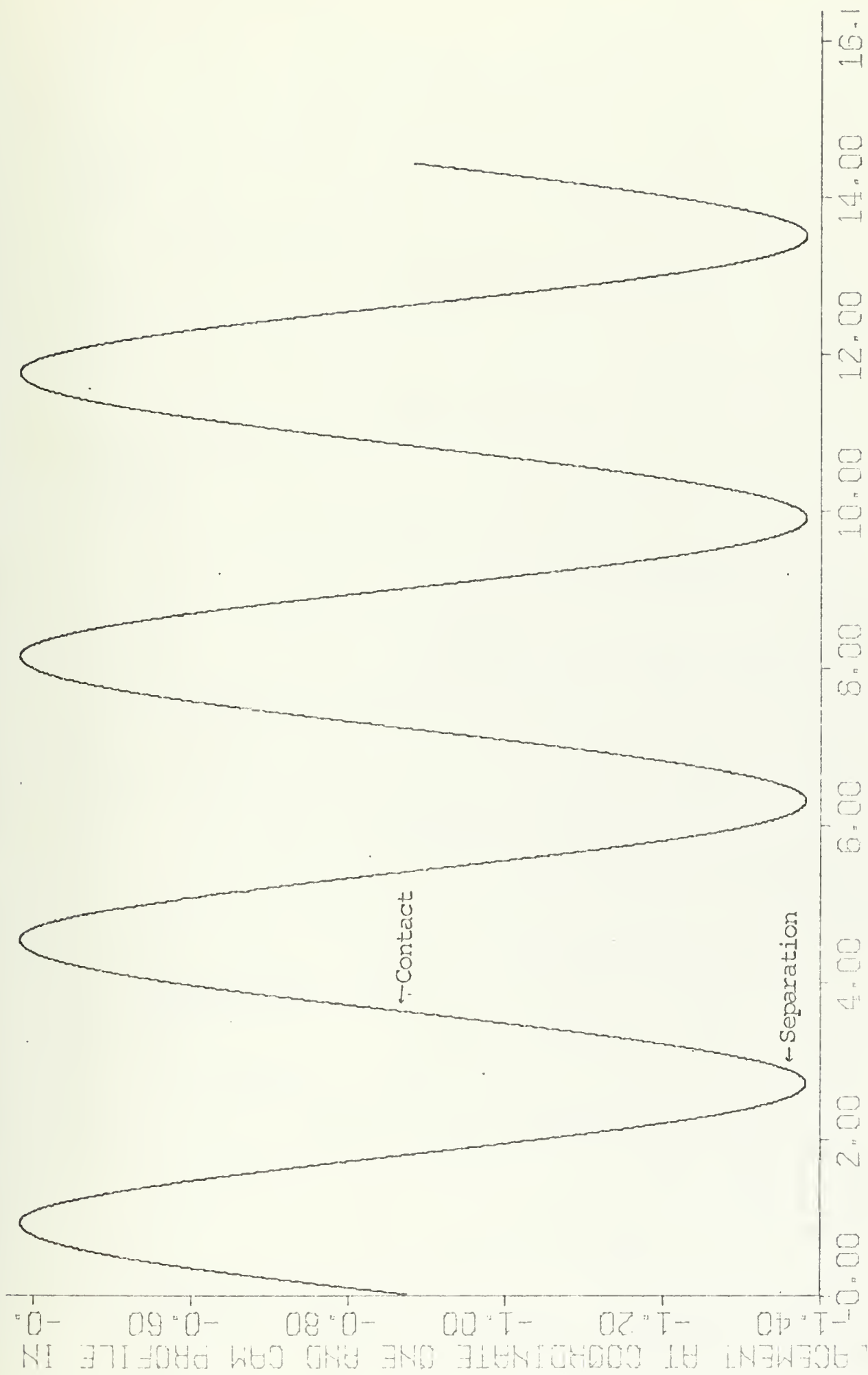addition, the impact force of collision between the two will increase.

42
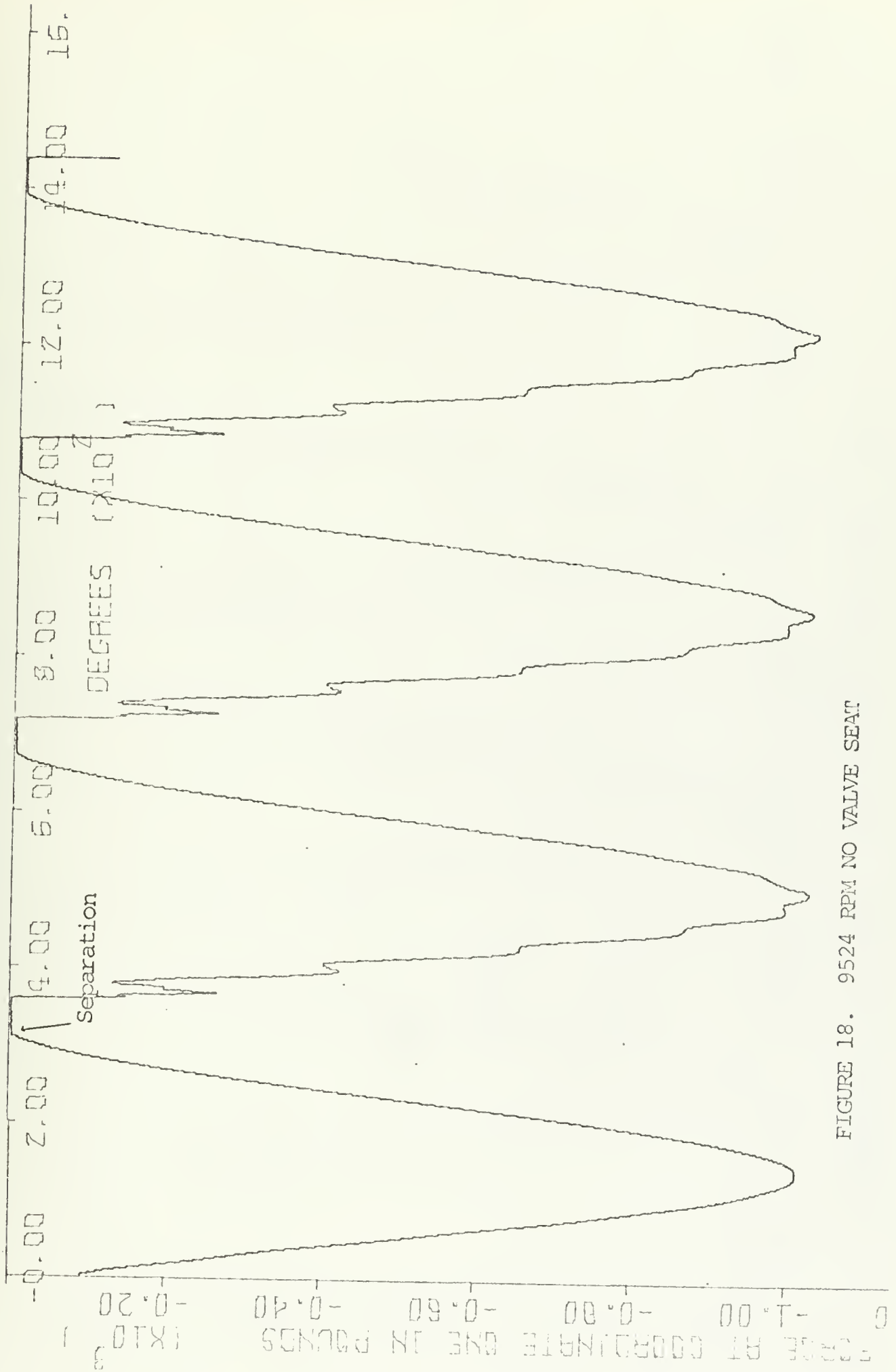
FIGURE 17. 9524 RPM N2 VALVE SEAT
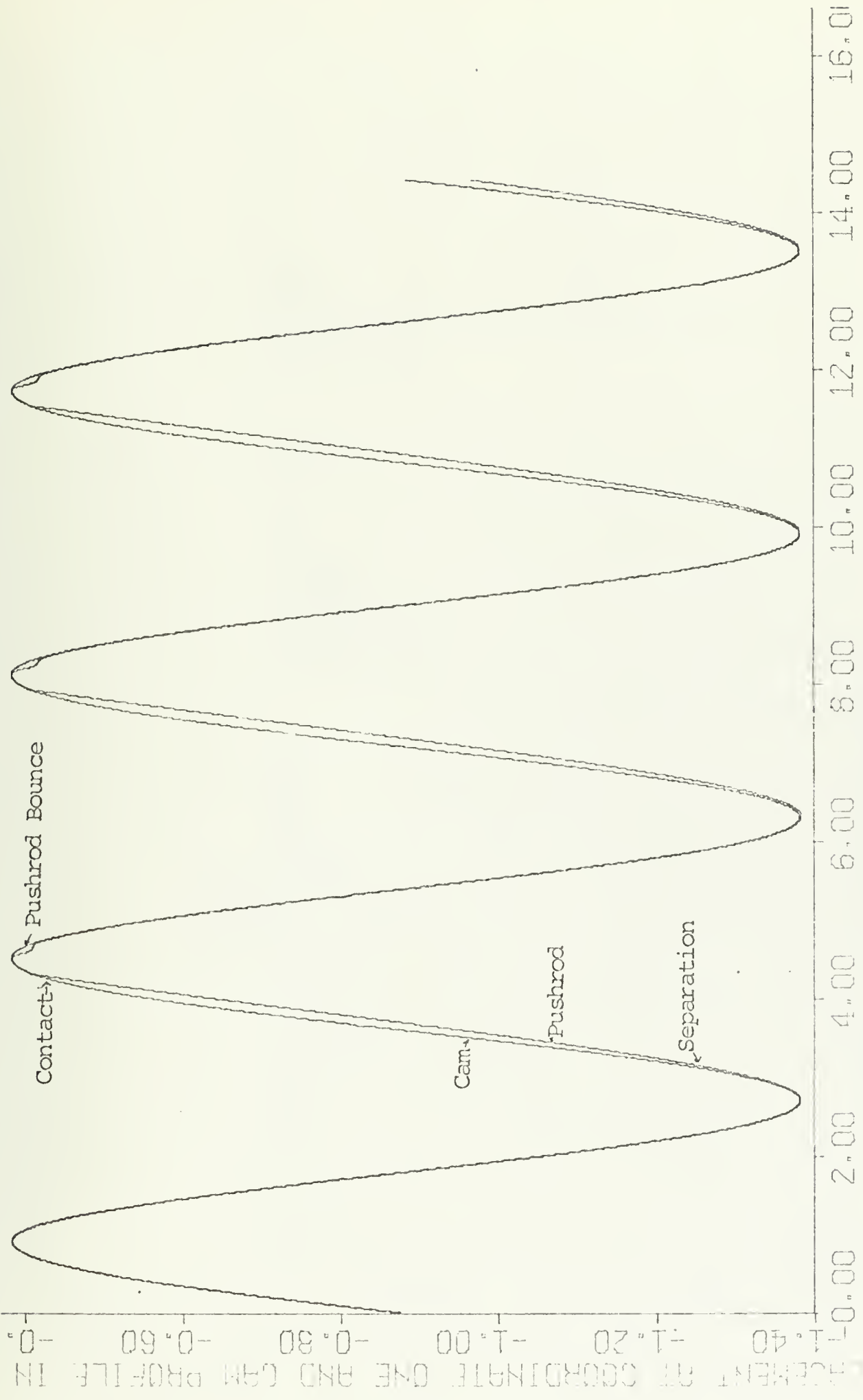
43

FIGURE 18. 9524 RPM NO VALVE SEAT

44

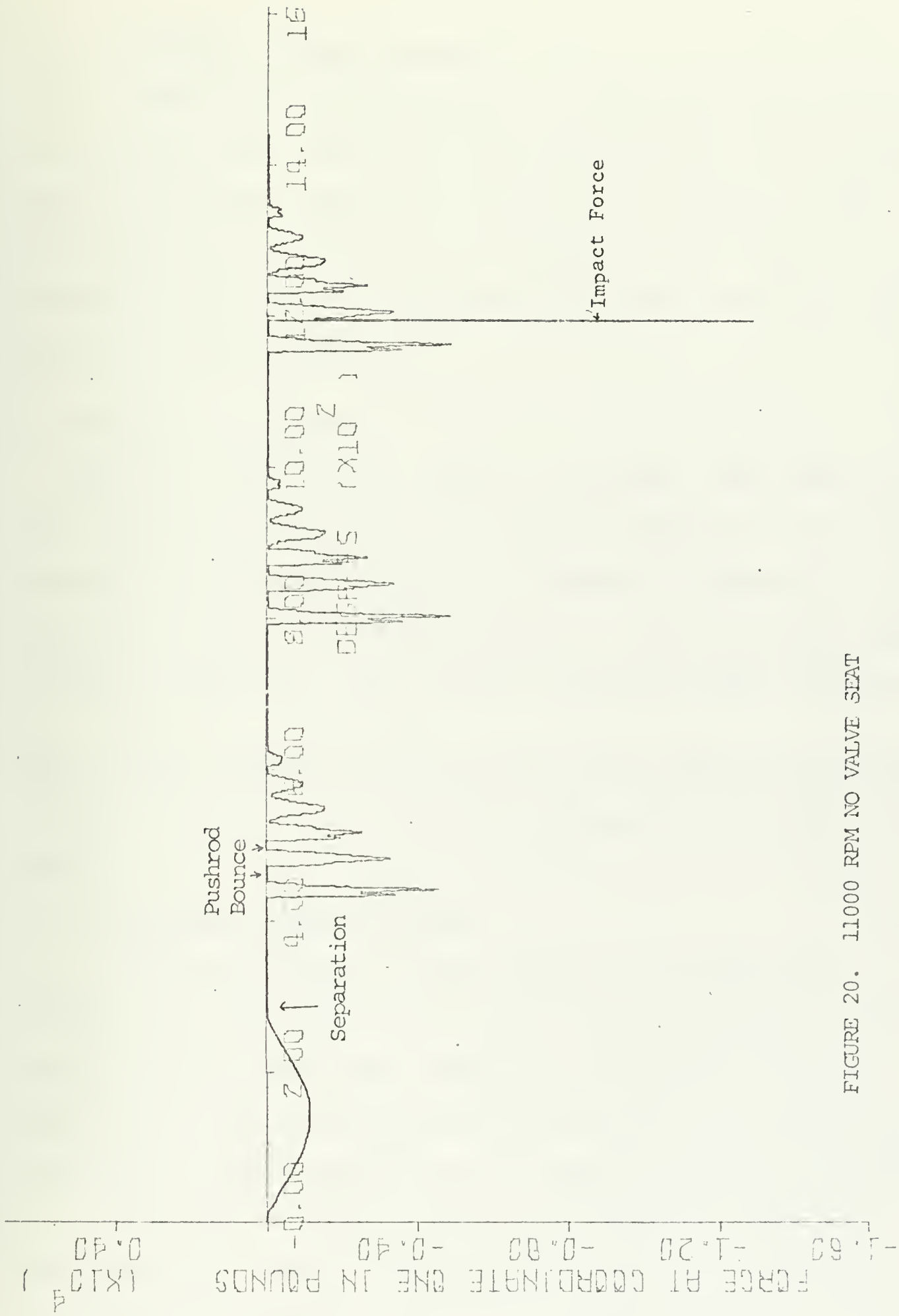FIGURE 19.   11,000 RPM NO VALVE SEAT

FIGURE 20. 11000 RPM NO VALVE SEAT

46

4.   20000 RPM - Figures 21 and 22

In this case it can be seen that once the pushrod loses contact
with the cam it never does come back in contact to remain. What takes
place is a continuous bouncing as the pushrod and cam come in contact
and the pushrod is thrown off again. The period of time that the two
do remain in contact is the time of take up of system inertia before the
pushrod is thrown off again.

B.   WITH VALVE SEAT INCLUDED

Next a valve seat will be included in the system. Upon impact, $\dot{q}_7$
and $\ddot{q}_7$ are solved by the technique explained in Chapter IV, and the force
between the valve and valve seat, F_7, is evaluated by Equation 27. $\dot{q}_7$
takes one time step, ΔT, to reach a value of 0. $\ddot{q}_7$ takes one time step
to reach the value $(\dot{q}_{7_{t_2}} - \dot{q}_{7_{t_1}}) / \Delta T$ and another time step to reach the
value of zero. This means that F_7 at time t_2 will usually be higher than
the value at t_3 or t_1. Again this is to be expected at the moment of
impact.

1.   1000 RPM - Figures 23 and 24

As shown in Figures 17 and 18, until the cam reaches about
9500 RPM, the pushrod will remain in contact with the cam if the model
does not include a valve seat. Therefore, at 1000 RPM with a valve
seat, any loss of contact between the cam and pushrod will be caused by
the valve seat interference and not as a result of excessive cam speed.

Figure 23 represents the response of the pushrod to the valve
seat interference. Figure 24 gives the force at coordinate one, F_1 ,
and the force at coordinate seven, F_7 . On Figure 23 the cam and pushrod
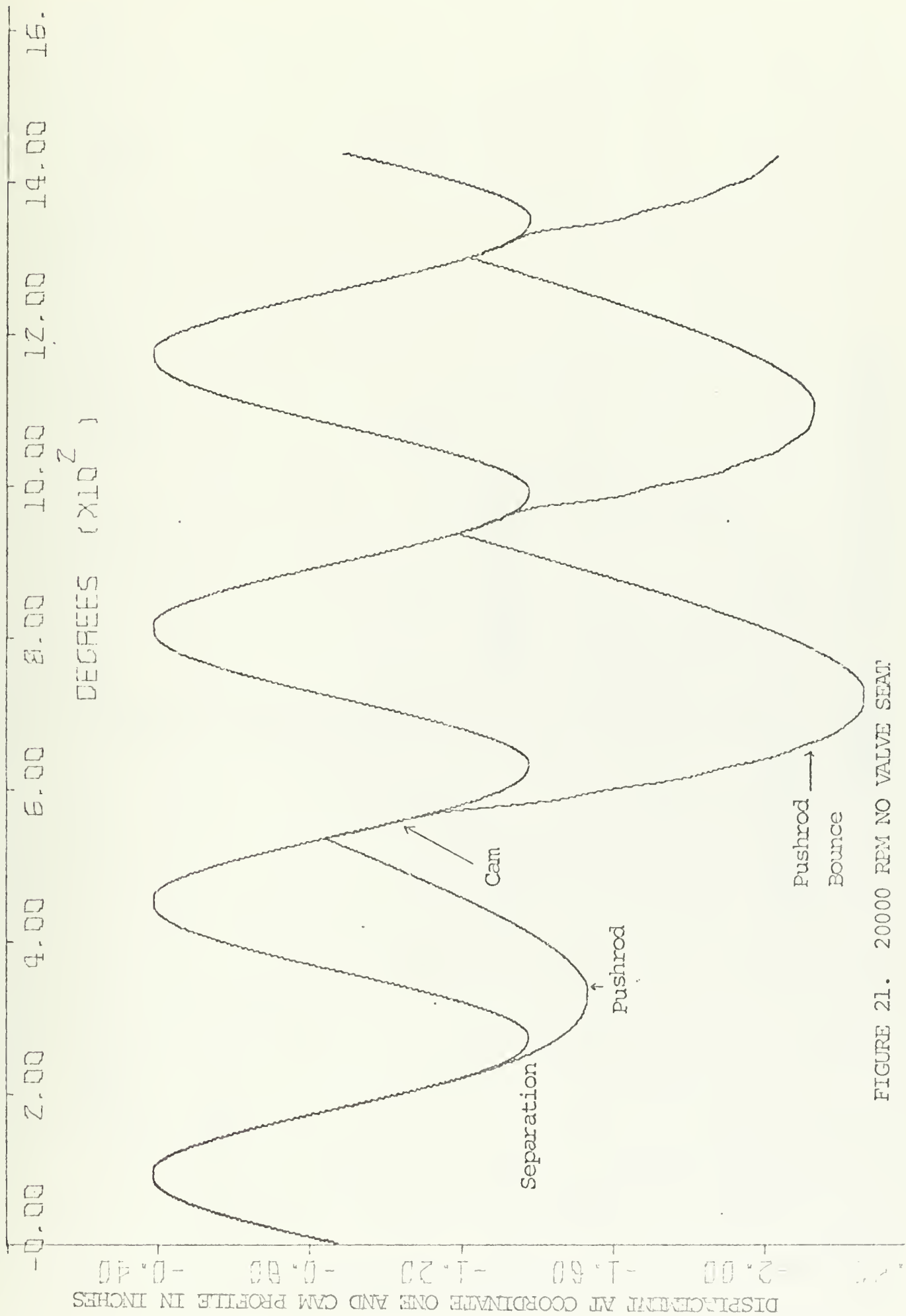profiles are superimposed until the valve comes in contact with the valve
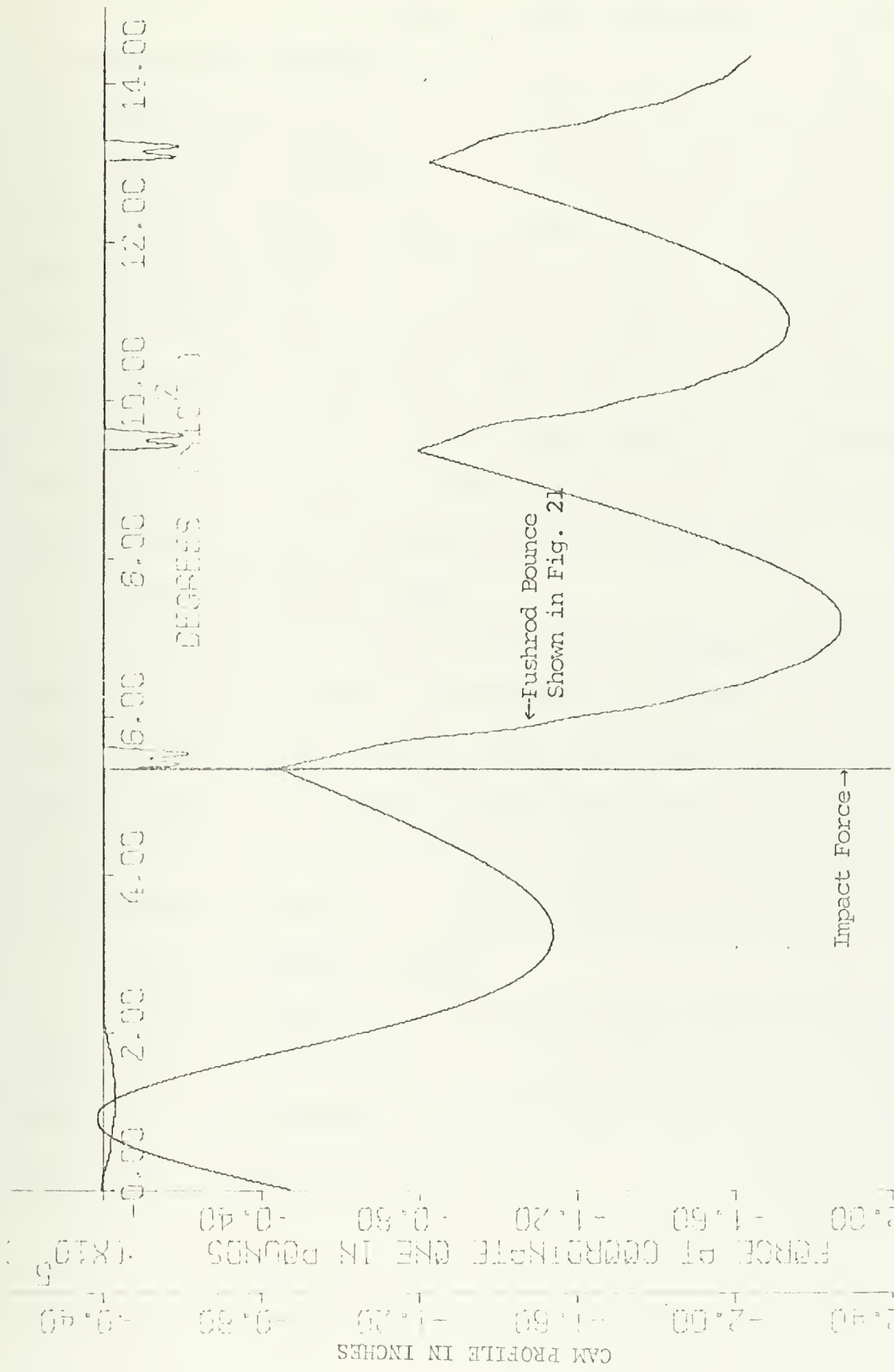
47

FIGURE 21. 20000 RPM NO VALVE SEAT

FIGURE 22. 20000 RPM NO VALVE SEAT

←Pushrod Bounce
Shown in Fig. 21

Impact Force→

FORCE AT COORDINATE ONE IN POUNDS (X10⁵)

DEGREES

CAM PROFILE IN INCHES

49

seat. This contact is transferred through the mechanism and the pushrod is pulled from the cam surface. In Figure 24 the upper curve is of F_1 and the lower curve is of F_7. Notice that during the period of contact at the valve only, F_7, oscillates and F_1 is equal to zero. The reverse takes place when the cam comes back in contact with the pushrod. F_1 oscillates and F_7 goes to zero. The force curves contrasted against each other give the best representation of the particular point or points of contact of the mechanism. When either force curve equals zero this indicates no contact at that particular coordinate. In addition, as will be shown for faster cam speeds, bounce of both the valve and pushrod takes place and is identifiable on the force curves.

2. 5000 RPM - Figure 25 and 26

This is a faster version of the previous example. The force curves are of interest due to the oscillation upon impact. In this case, as evidenced by the additional flat areas on the F_1 and F_7 curves, there are bounces of the pushrod and valve after impact. Also of interest in Figure 25 is the indication of the increased oscillation of the displacement of the pushrod after separation from the cam.

3. 9000 RPM - Figures 27 and 28

Everything stated previously is even more in evidence at this speed. Figure 28 indicates several bounces of the pushrod and valve after impact. The oscillation of q_1 on Figure 27, after the pushrod loses contact, is more pronounced.
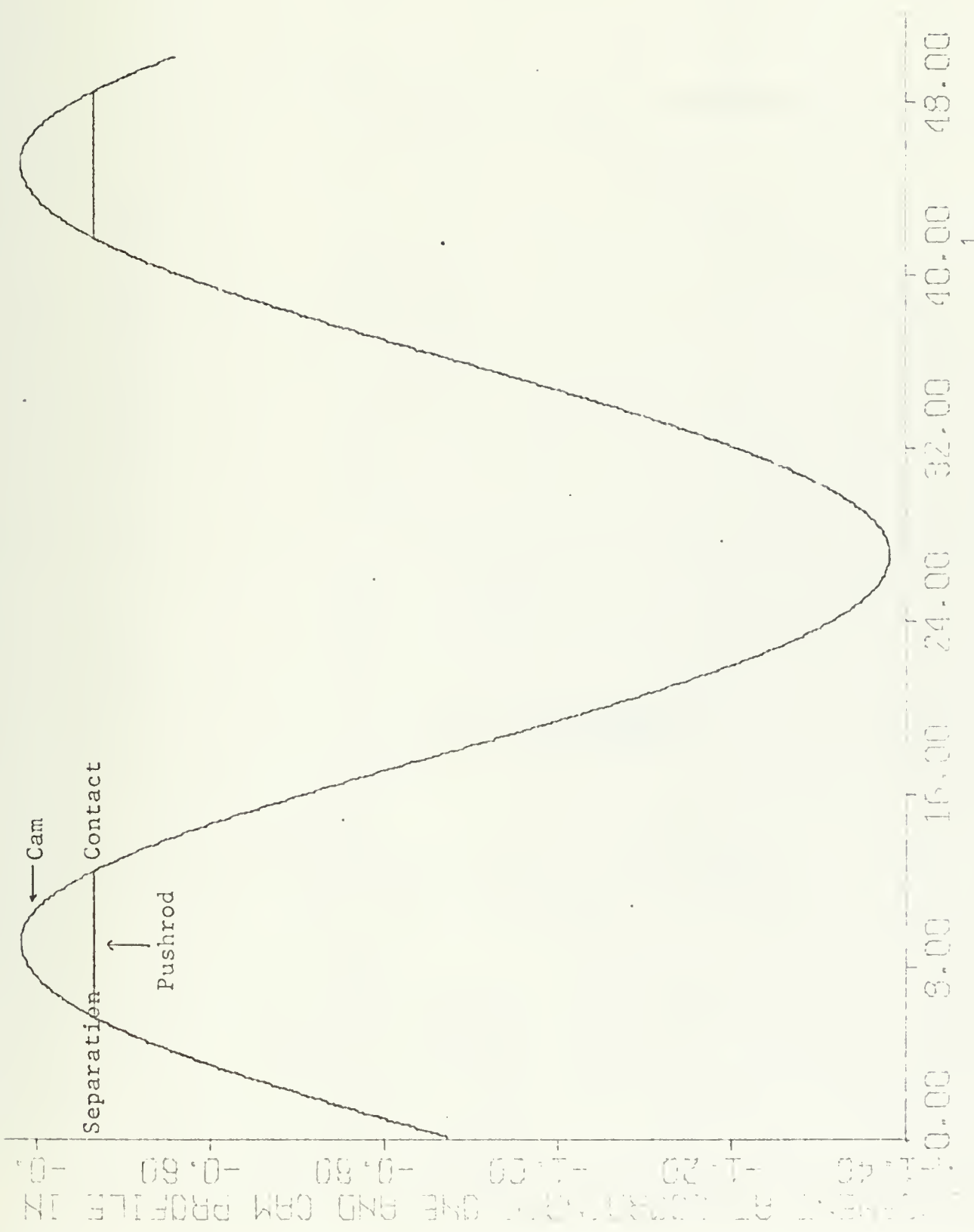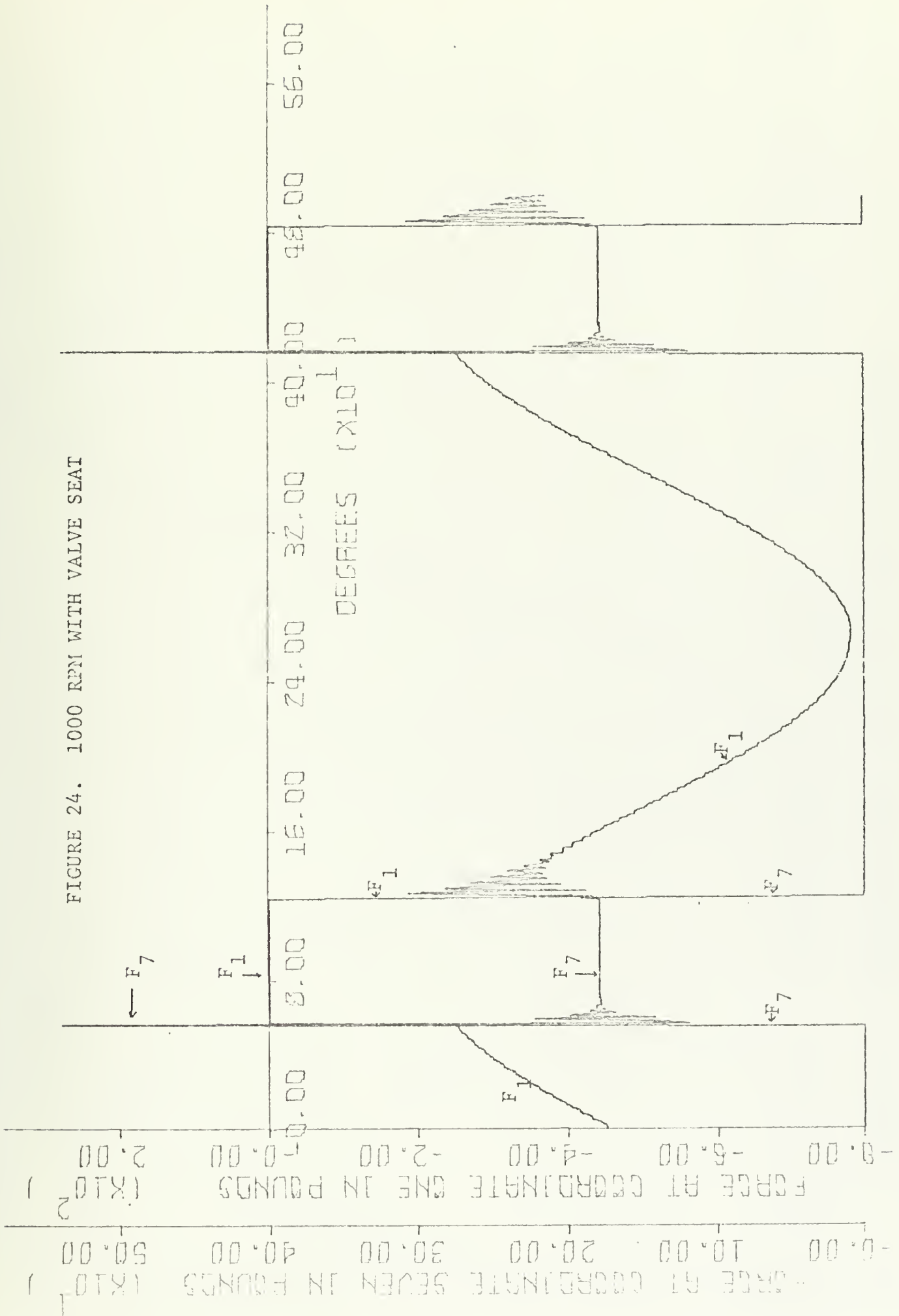
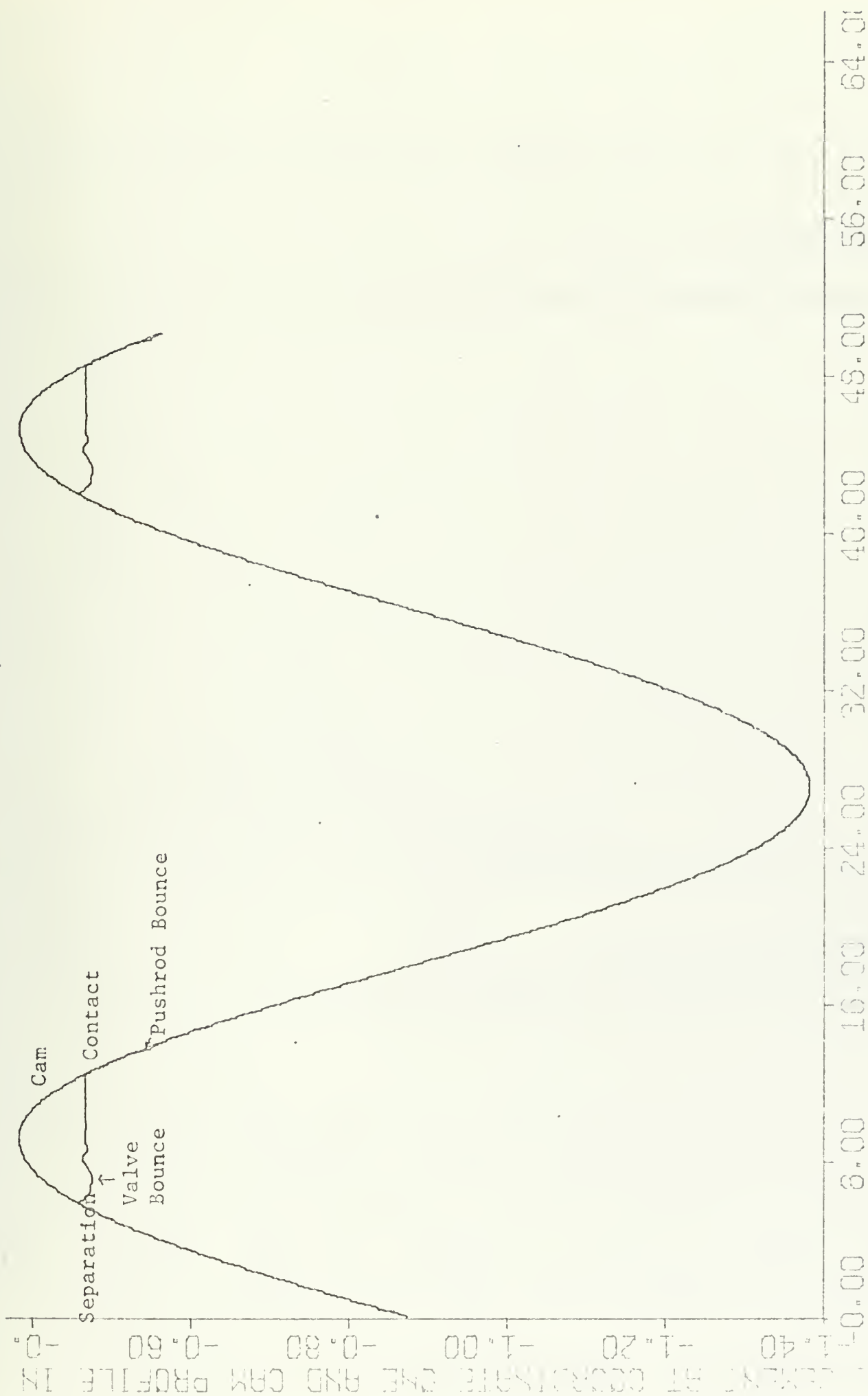FIGURE 23. 1000 RPM WITH VALVE SEAT

FIGURE 24. 1000 RPM WITH VALVE SEAT

52

FIGURE 25. 5000 RPM WITH VALVE SEAT

Cam

Contact
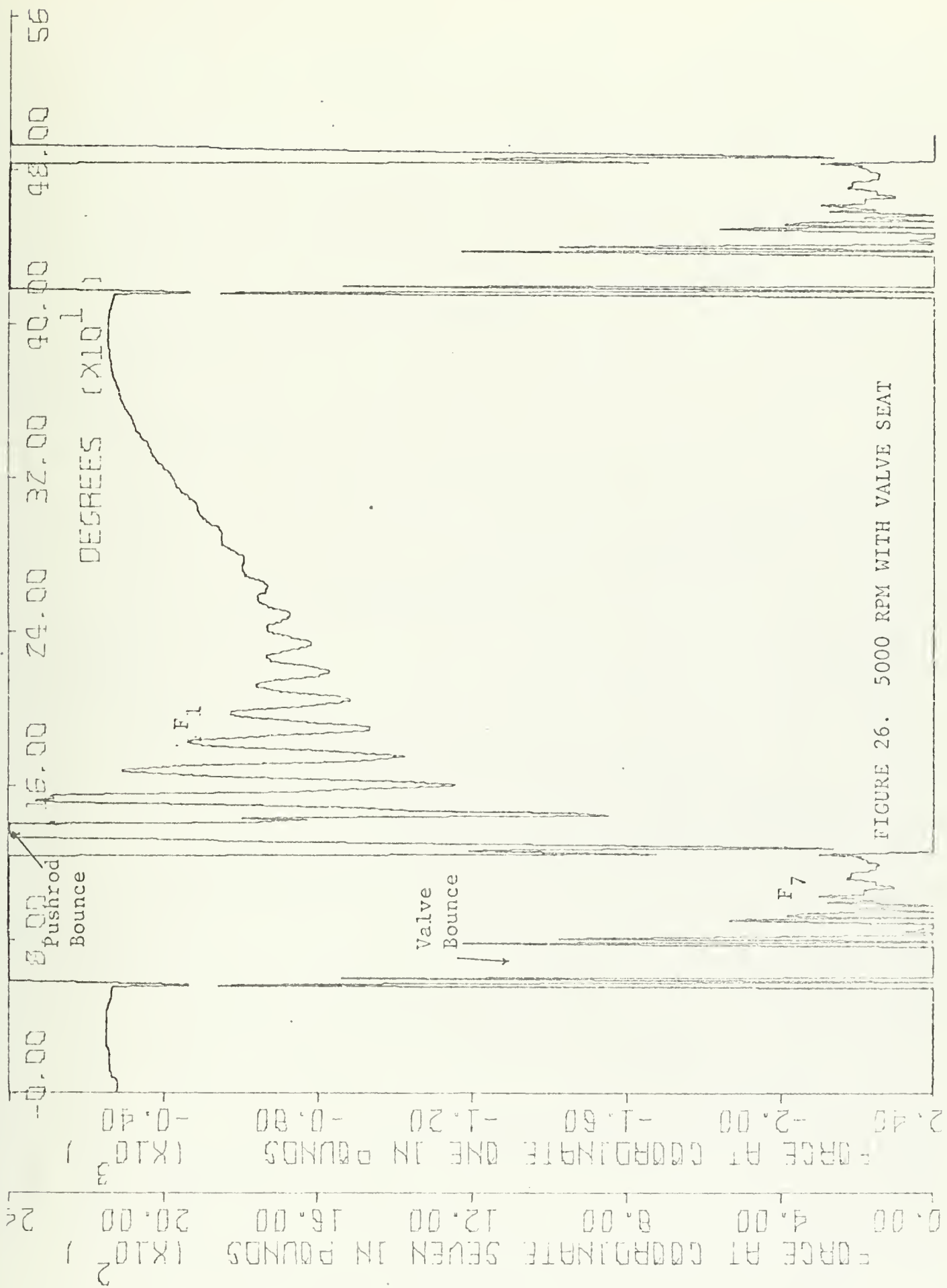
Pushrod Bounce

Separation

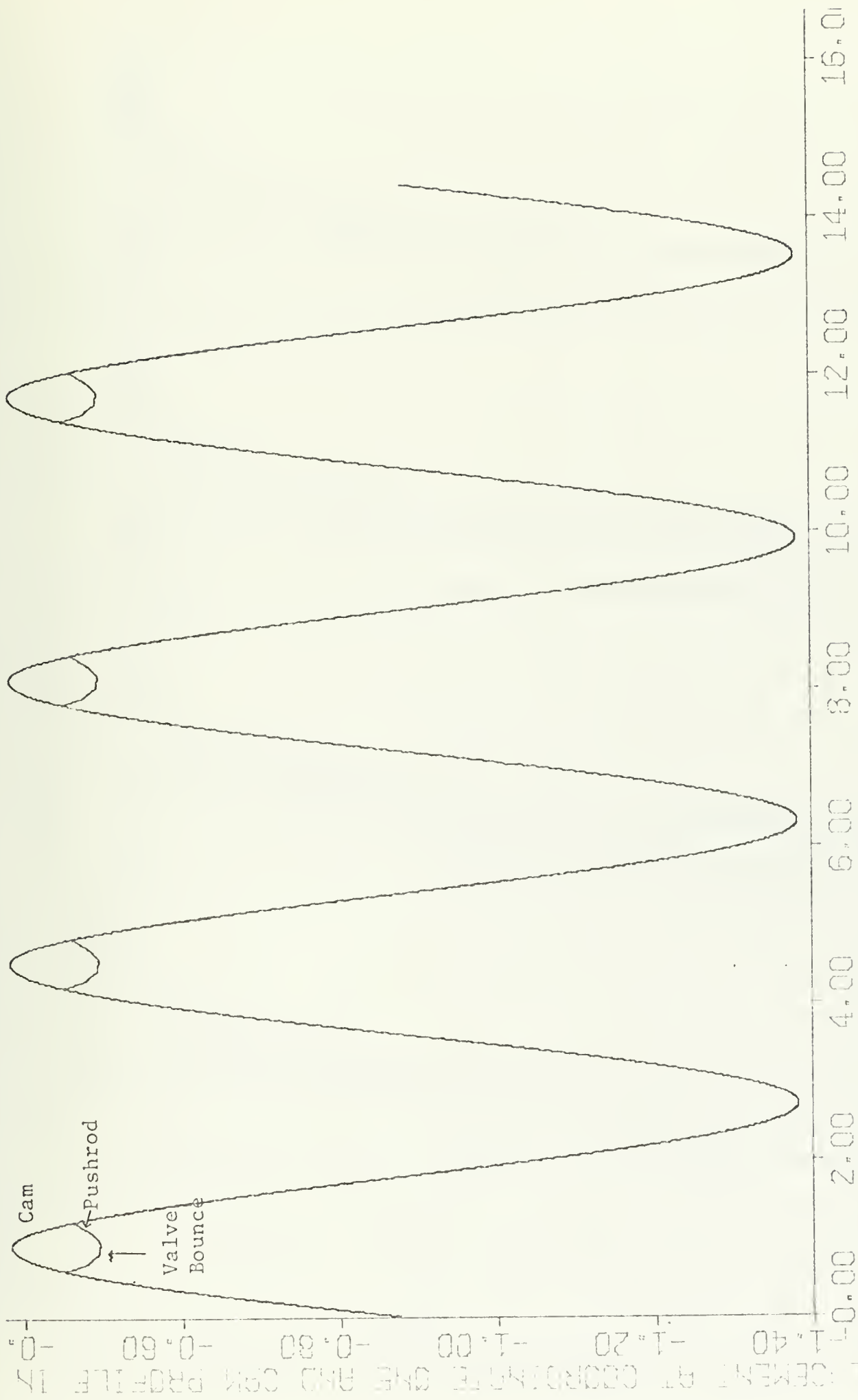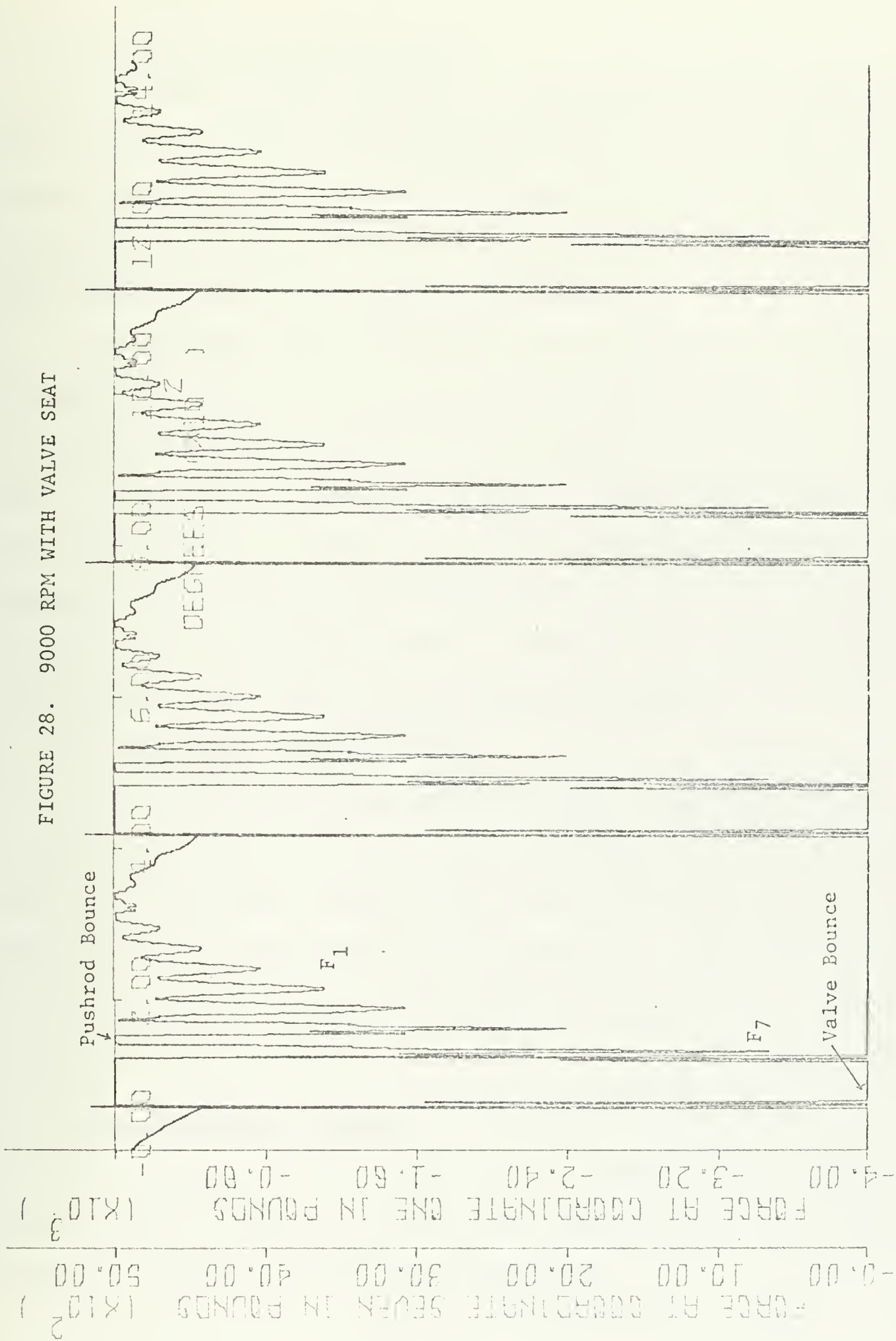Valve
Bounce

FIGURE 26. 5000 RPM WITH VALVE SEAT

54

FIGURE 27. 9000 RPM WITH VALVE SEAT

FIGURE 28. 9000 RPM WITH VALVE SEAT

4. 13205 RPM – Figures 29 and 30

The speed is above 9500 RPM so it can be expected that the valve seat and excess speed will have interacting effects on the model. Of interest is what happens first when the system is floating free of external forces – will the cam come in contact with the pushrod before the valve comes in contact with the valve seat?

The pushrod first loses contact with the cam due to the action of the valve on the valve seat. The cam and pushrod come back in contact, the force F_1 oscillates, and the pushrod bounces and is finally thrown free. At just before 460 degrees, as shown by Figure 30, the valve comes in contact with the valve seat. Just after 480 degrees the pushrod also comes in contact with the cam and the system is subsequently thrown free again. In this case when the system is floating free of external forces the valve seat comes back in contact before the pushrod.

5. 20000 RPM – Figures 31 and 32

The pushrod again first loses contact due to the valve seat interaction, comes back in contact with the cam, and is thrown free again. From then on the system resembles that shown on Figure 21 since the valve does not come in contact with the valve seat again. The pushrod continues to bounce on the cam at such a height that the valve does not reach the position of the valve seat.

C. RELATED PROBLEMS OF INTEREST

The previous examples have shown the more routine results obtainable with the model. Figures 33 through 41 are graphs of some of the additional situations imposed on the model for examination.
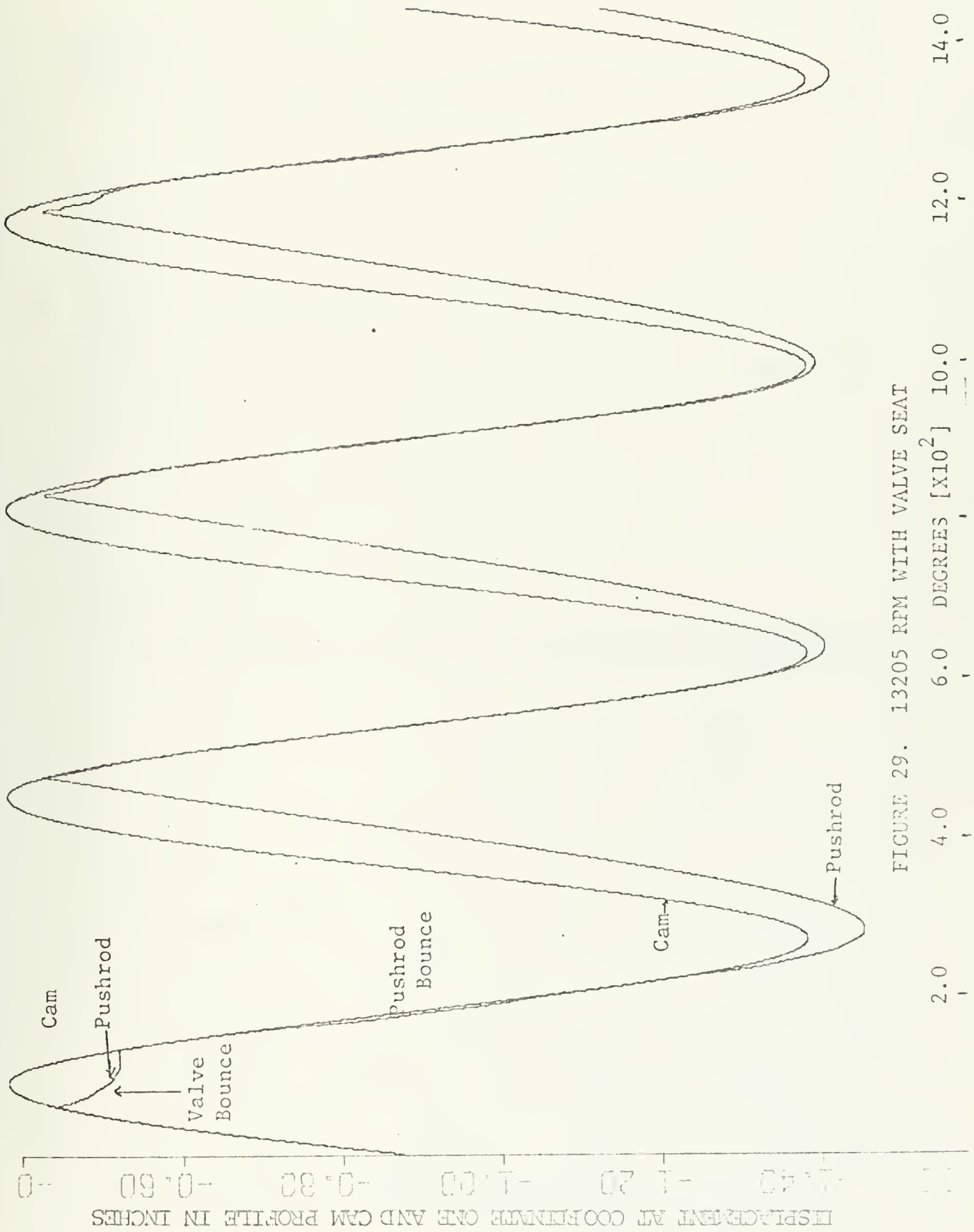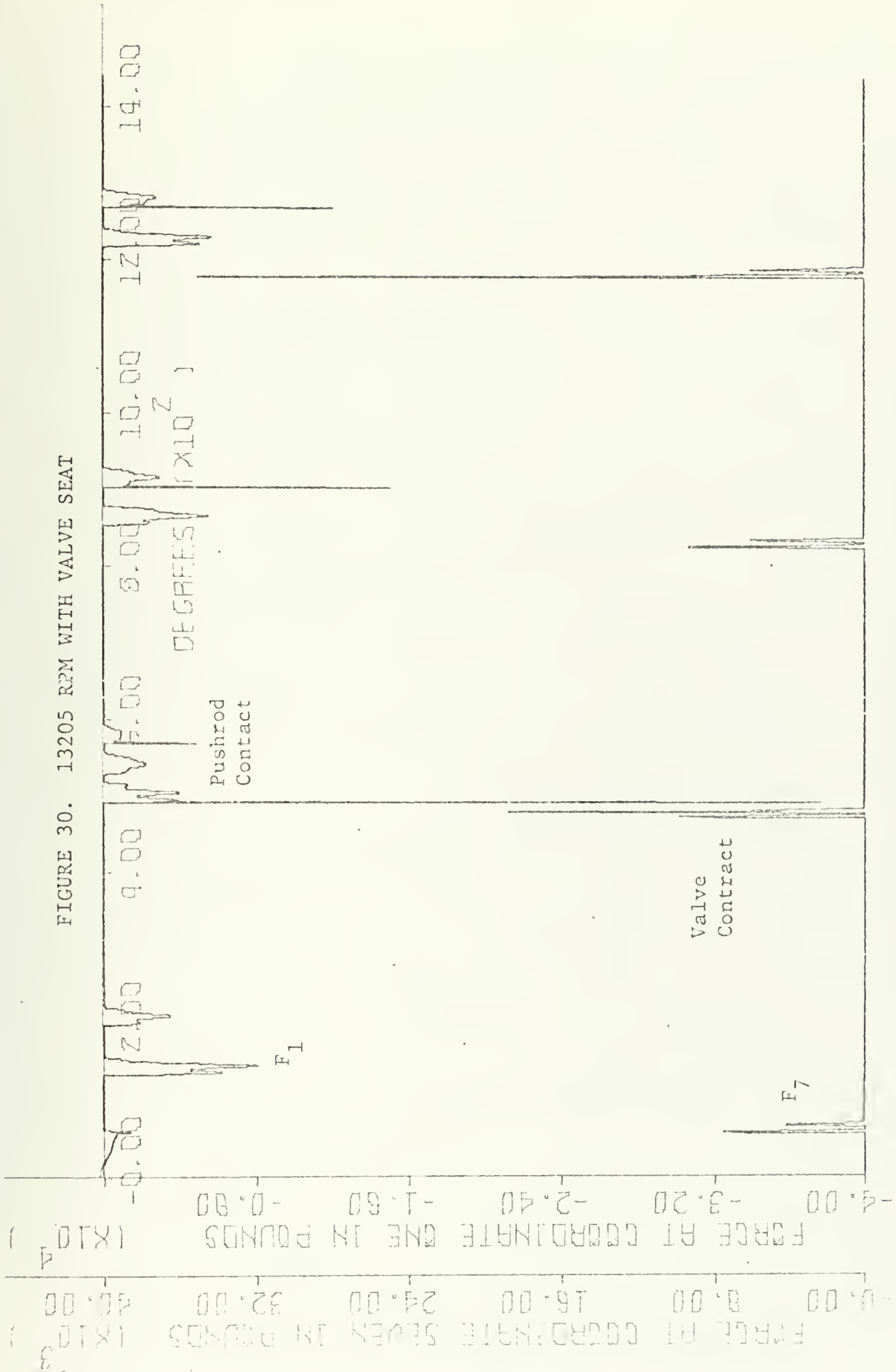
FIGURE 29. 13205 RPM WITH VALVE SEAT

DISPLACEMENT AT COORDINATE ONE AND CAM PROFILE IN INCHES

DEGREES [x10^2]

FIGURE 30. 13205 RPM WITH VALVE SEAT
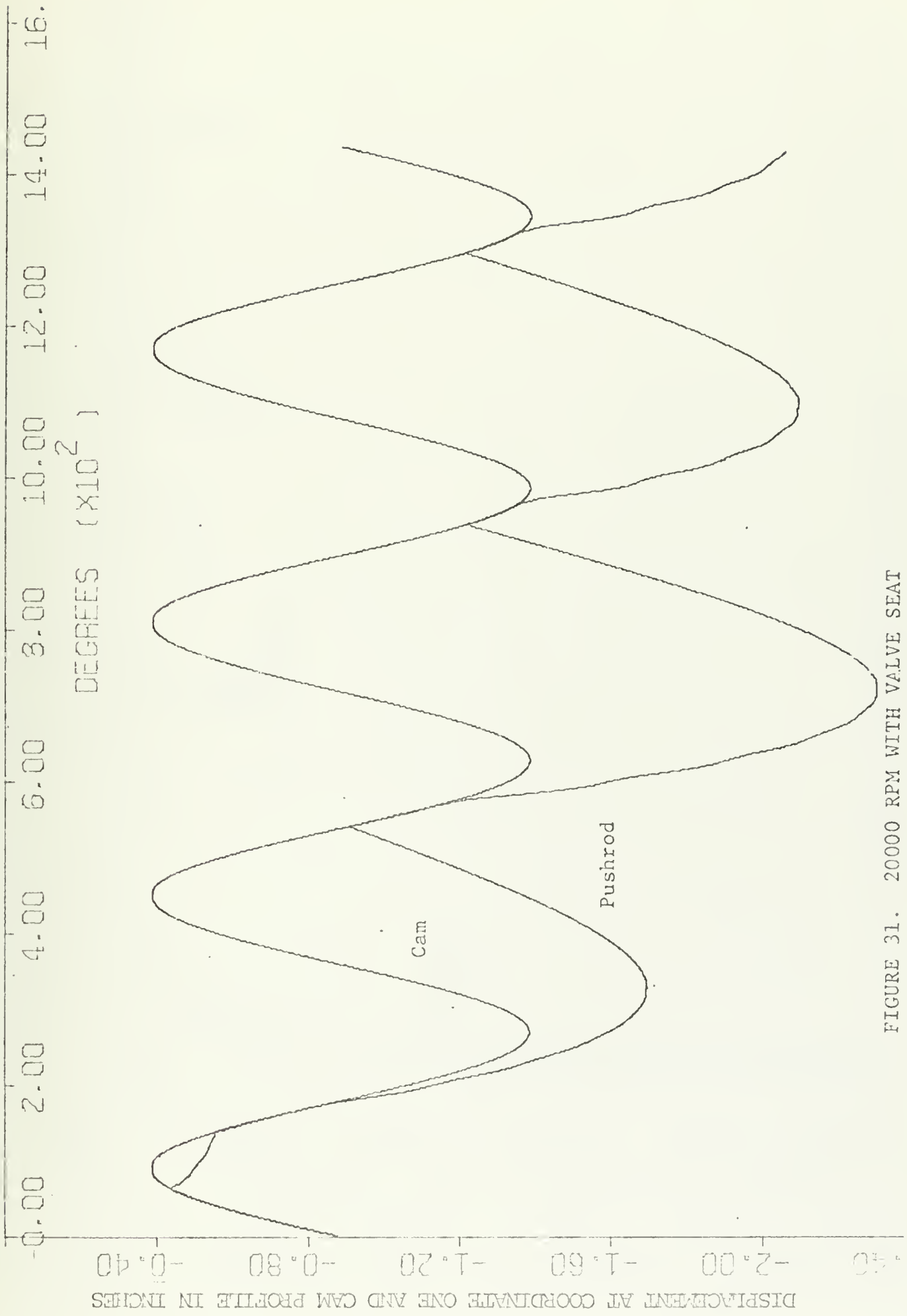
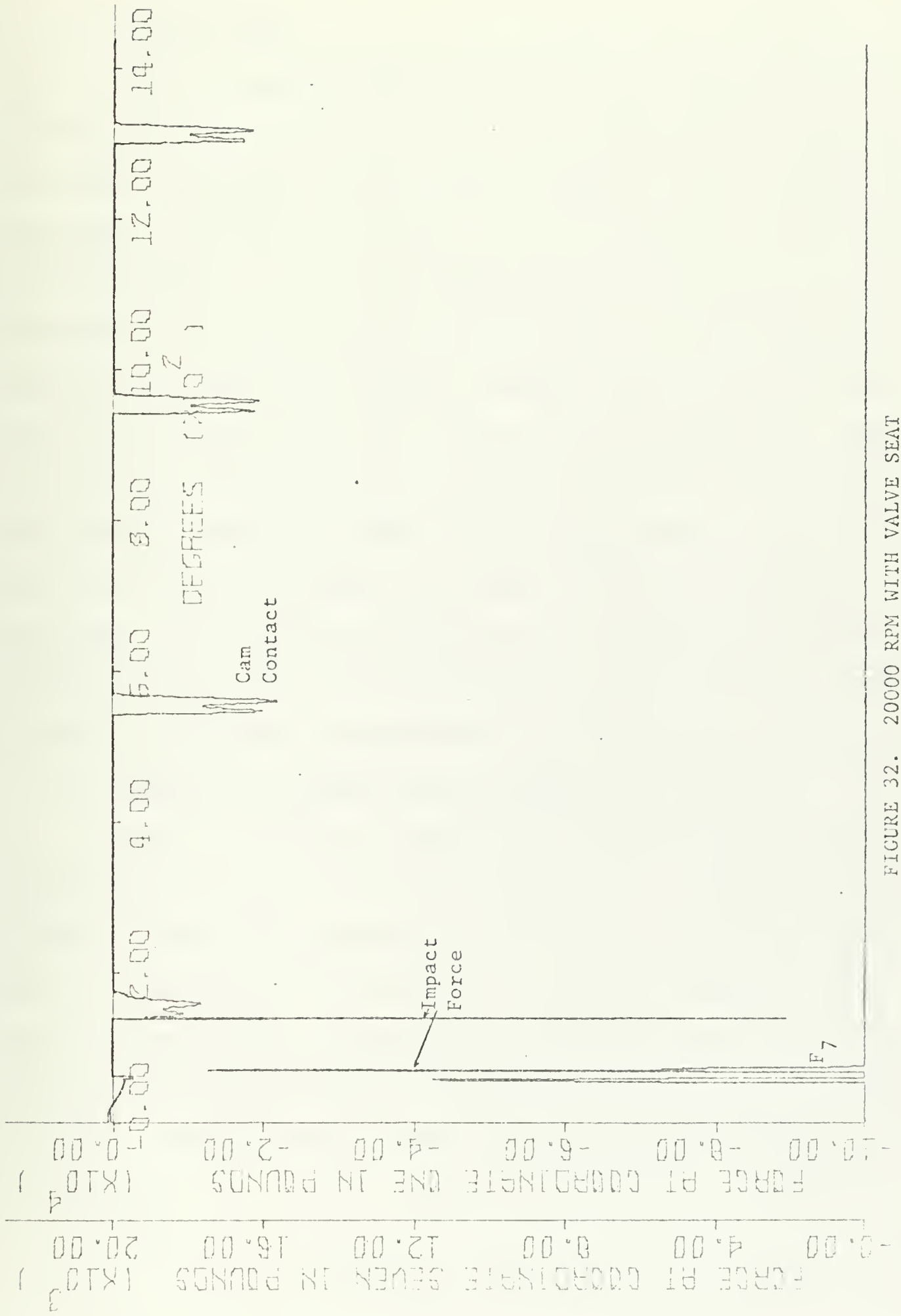FIGURE 31. 20000 RPM WITH VALVE SEAT

FIGURE 32.   20000 RPM WITH VALVE SEAT

61

1. <u>Machining Error</u>

Figure 33 represents what happens due to a small machining error
on the cam surface. The error was beteeen 268 degrees and 272 degrees.
The value of cam displacement was assumed constant and the cam velocity
and acceleration taken equal to zero. The best indication of the results
of the flat space is given by the oscillation of the force profile. On
all graphs data points were plotted every degree. For this reason, this
graph does not indicate the complete response. When the pushrod comes
up to or goes off the flat space it hops off the cam surface for a small
period of time, about .75 degrees, and then comes back to the cam surface.
This should be indicated on Figure 33 by the force going to zero. Since
this occurs between successive data points it does not get plotted on
the graph. The oscillation of the force at coordinate one on Figure 33
indicates problems that could be associated with several machining errors
on the same cam surface. The machining error here is 0.0003 inches.

2. <u>Undamped at the Lowest Natural Frequencies - Figure 34</u>

Figure 34 is the force between the cam and pushrod, F_1 , for the
model without damping. This graph substantiates the value of the lowest
natural frequency, 691.radians/sec. or 6602.5 RPM, of the undamped model.
This value from Figure 14 was obtained by solution of Equation 14 for
the eigenvalue problem. At the resonance frequency of 6602.5 RPM it
takes very little force above the static value to cause the mechanism
to operate. As can be seen on Figure 34 the force oscillates about
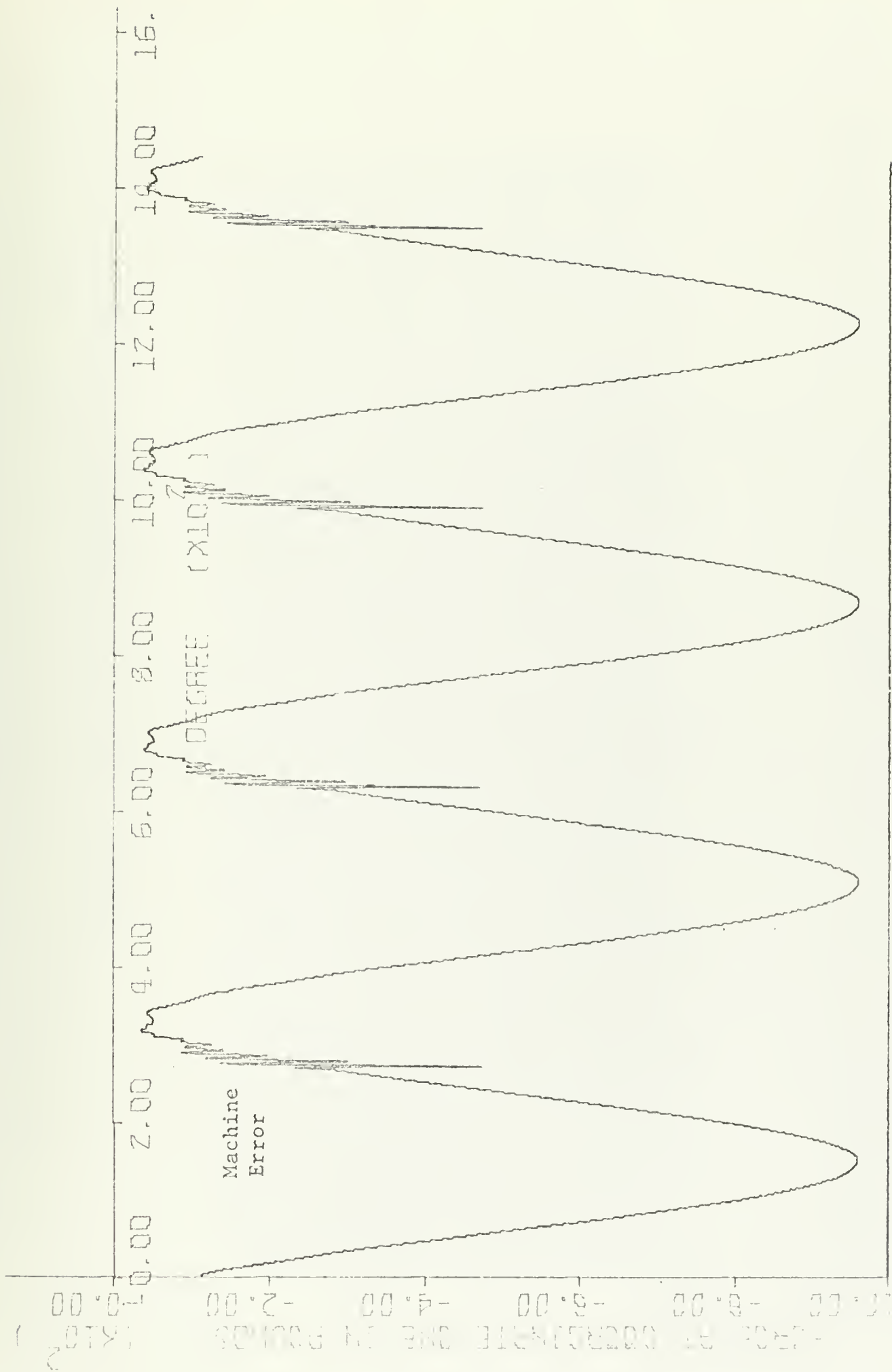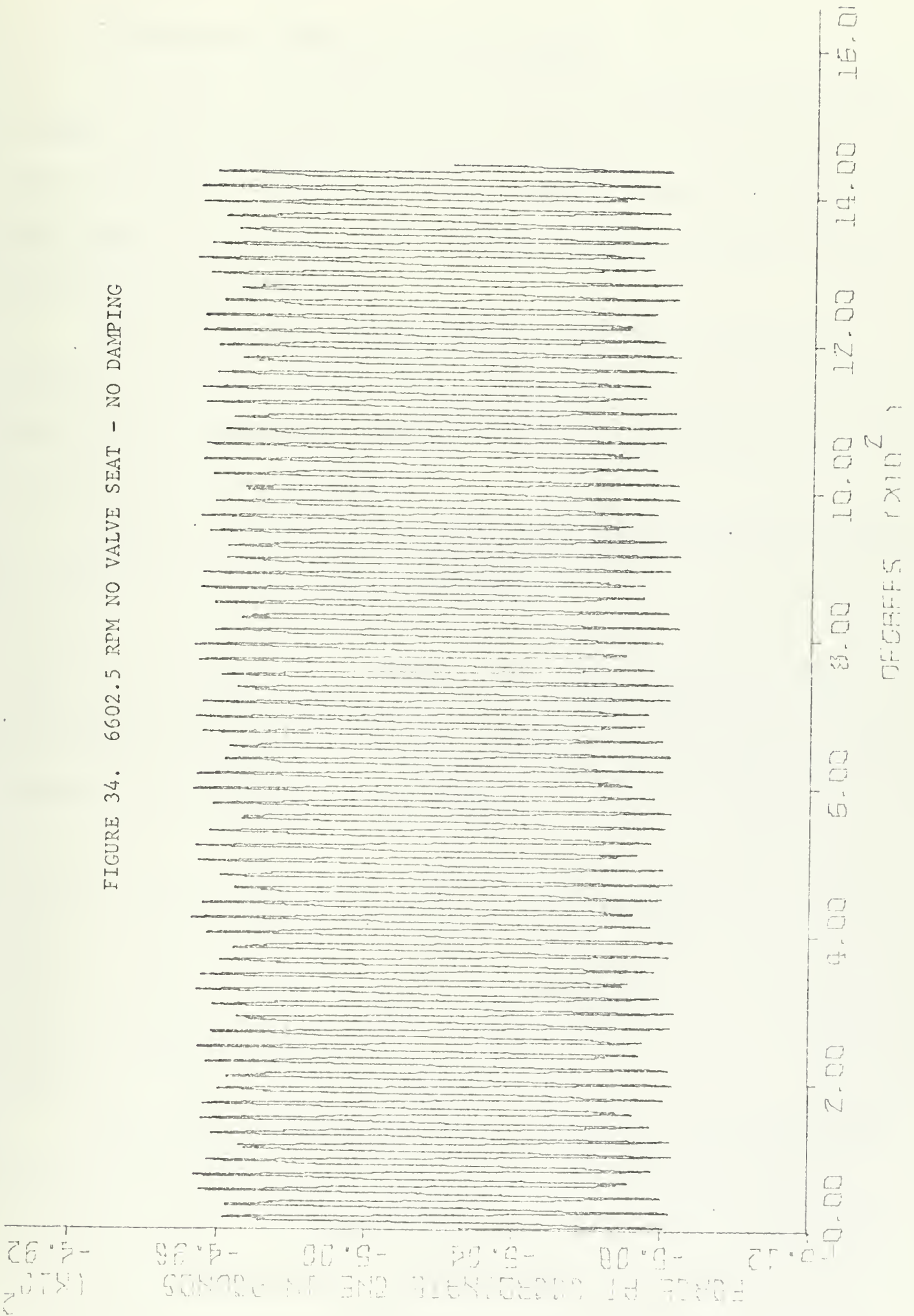10 pounds.

FIGURE 33. 9000 RPM MACHINING ERROR

63

FIGURE 34.   6602.5 RPM NO VALVE SEAT - NO DAMPING

3. Polydyne Cam Profile - Figures 35 and 36

Up to this point all the cam profiles have been harmonic, with no dwell, and represented by .5 sin (ωt) inches with ω equal to the value of cam speed in radians per second. Polydyne cam profiles are quite popular and this next example examines different responses of the mechanism to polydyne profiles.

There are several references that are good on development of polydyne cam profiles, (4), (10), (11), and (12). It is not the intent here to develop this theory, but just to outline how the profile was set up for solution on the model.

Basically all that is needed for model input is $\dddot{q}_1$, $\ddot{q}_1$, $\dot{q}$, and q_1. With this in mind a polynomial equation,

$$q_1 = C_0 + C_1\theta + C_2\theta^2 + C_3\theta^3 + C_4\theta^4 + C_5\theta^5 + C_6\theta^6 + C_7\theta^7 , \qquad (29)$$

was written with θ equal to the angle of rotation of the cam in degrees. Differentiating for $\dot{q}_1$, $\ddot{q}_1$, and q gives,

$$\dot{q}_1 = C_1 + 2C_2\theta + 3C_3\theta^2 + 4C_4\theta^3 + 5C_5\theta^4 + 6C_6\theta^5 + 7C_7\theta^6 , \qquad (30)$$

$$\ddot{q}_1 = 2C_2 + 6C_3\theta + 12C_4\theta^2 + 20C_5\theta^3 + 30C_6\theta^4 + 42C_7\theta^5 , \qquad (31)$$

$$\dddot{q}_1 = 6C_3 + 24C_4\theta + 60C_5\theta^2 + 120C_6\theta^3 + 210C_7\theta^4 . \qquad (32)$$

The initial conditions were taken to be $\dot{q}_1$, $\ddot{q}_1$, and $\dddot{q}_1$ equal to zero at the beginning and end of the stroke. The value of q_1 at the beginning and end of the stroke would be specified. The one restriction placed on this situation was that the pushrod was not allowed to leave the surface of the cam at any time regardless of the value of the force at coordinate one.

Taking θ equal to zero as the beginning of the stroke, C_1, C_2, and C_3 are seen to be zero due to the initial values of q_1, $\dot{q}_1$, and $\ddot{q}_1$. C_0 equals the initial value of q, and thus Equations 29 through 32 may be written in matrix form.

$$
\begin{Bmatrix} q_1 - C_0 \\ \dot{q}_1 \\ \ddot{q}_1 \\ \dddot{q}_1 \end{Bmatrix}
=
\begin{bmatrix}
\theta^4 & \theta^5 & \theta^6 & \theta^7 \\
4\theta^3 & 5\theta^4 & 6\theta^5 & 7\theta^6 \\
12\theta^2 & 20\theta^3 & 30\theta^4 & 40\theta^5 \\
24\theta & 60\theta^2 & 120\theta^3 & 210\theta^4
\end{bmatrix}
\begin{Bmatrix} C_4 \\ C_5 \\ C_6 \\ C_7 \end{Bmatrix}
\tag{33}
$$

The unknown coefficients, C_4, C_5, C_6, and C_7 can now be solved for by substituting $q_1 = q_{1_F}$, and $\dot{q}_1 = \ddot{q}_1 = \dddot{q}_1 = 0$, the values at the end of the stroke, into Equation 33.

$$
\begin{Bmatrix} q_1 |_F - C_0 \\ 0 \\ 0 \\ 0 \end{Bmatrix}
\tag{34}
$$

where $q_1 |_F$ indicates the value of q_1 at the end of the stroke. Using Equation 34 and the value of θ at the end of the stroke in Equation 33, C_4, C_5, C_6, and C_7 can be found. With C_4, C_5, C_6, and C_7 known, the values of q_1, $\dot{q}_1$, and $\ddot{q}_1$ can now be solved for at any time within the stroke. A similar solution for a 345 polydyne profile can be made. However, only the initial and final values of q_1, $\dot{q}_1$, and $\ddot{q}_1$ need be defined.

66

Figure 35 shows the basic cam profile for both the 4567 profile and the 345 profile. Figure 35 also gives the response of the valve displacement q_7 to each of these profiles. Both cam profiles were taken to open in 90 degrees, to dwell for 90 degrees, to close in 90 degrees, and again to dwell for 90 degrees. This, in effect, simulates the inclusion of another cam at coordinate one so that the pushrod follows precisely the profile of the cam at all times, no matter what the value of F_1 might be.

Figure 36 gives an example of the response of the system when the amount of dwell is changed. A 4567 profile is simulated. The first run has a 90, 90, 90, 90 degree profile as previously described, but the second run takes 45 degrees to open, dwell for 45 degrees, close in 225 degrees and dwells for 45 degrees. Again this figure gives both cam and valve profiles.

4. 15000 RPM - Figures 37 to 41

It is of interest to examine the relative deflections of individual members of the mechanism for the harmonic cam previously used, $q = .5 \sin \omega t$.

Figures 37 to 39 represent the amount of deformation undergone by the model members during one particular operation. Figure 37 represents the axial deformation of the valve stem. Figure 39 indicates the amount of bending undergone by the rocker arm.

Figures 40 and 41 are the force and displacement graphs for 15000 RPM in the same manner as shown previously.
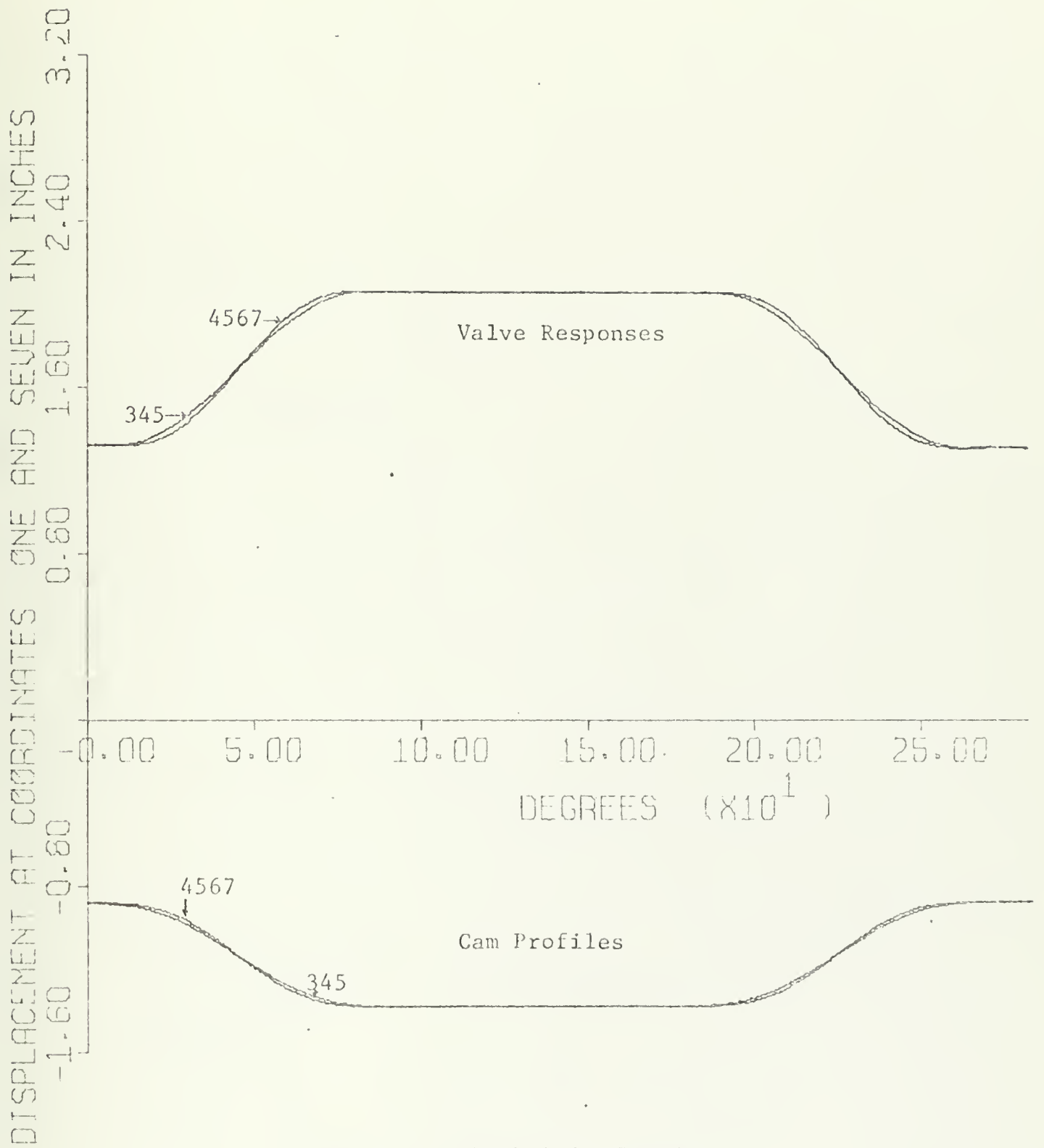
FIGURE 35. 8000 RPM
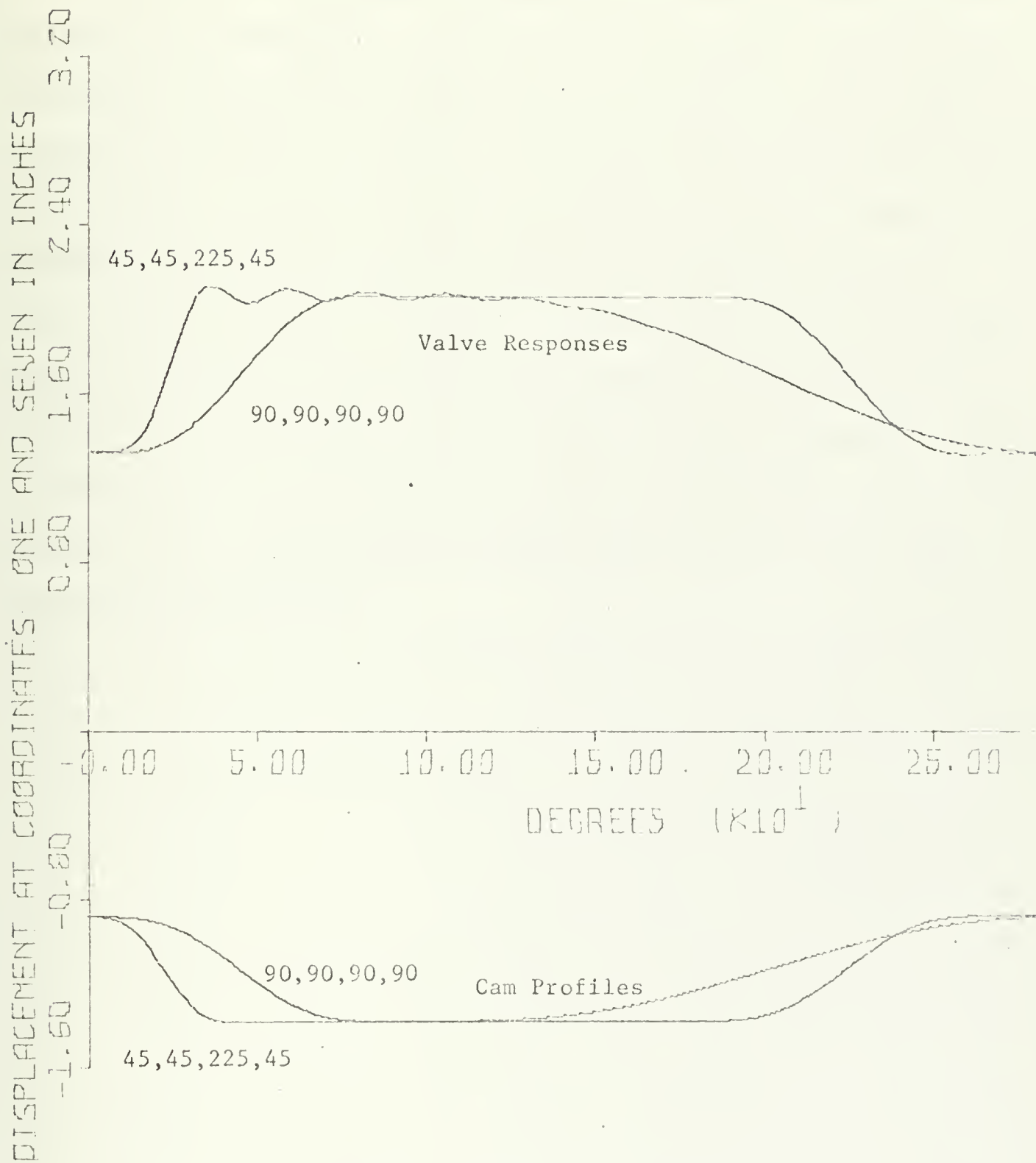
FIGURE 36. 8000 RPM

On Figure 41 at about 850 degrees it is shown that both the cam
and valve seat have come in contact with the mechanism. Careful exami-
nation shows that the cam contacts prior to the valve. In the length
of time it takes for the system to take up the inertia and be thrown off
the cam again, the valve also comes in contact with the valve seat. It
should be noted that 15000 RPM is between the 13205 RPM value of cam
speed where it was noted in Figure 29 that the valve hits the valve seat
before the pushrod hits the cam and the 20000 RPM value of cam speed
where the value never comes back in contact with the valve seat. As can
be seen in Figure 41 for 15000 RPM sometimes the valve does come in
contact, i.e., 850 degrees and at other times it doe not, i.e., 500
degrees and 1250 degrees.

FIGURE 37. 15000 RPM VALVE

FIGURE 38. 15000 RPM VALVE

72

FIGURE 39. 15000 RPM VALVE

FIGURE 40. 15000 RPM WITH VALVE SEAT

74
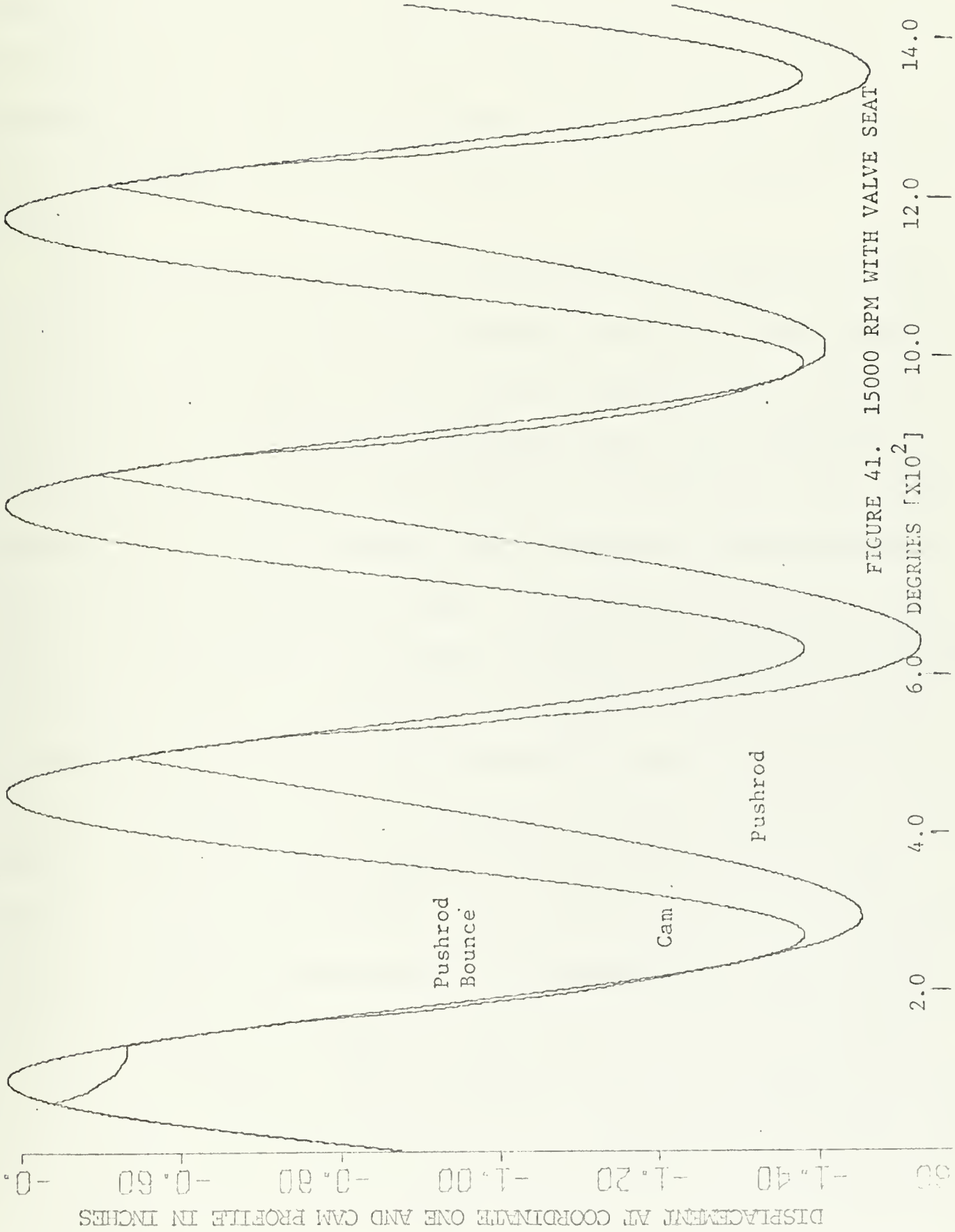
FIGURE 41. 15000 RPM WITH VALVE SEAT

75

VI. CONCLUSIONS

An elastic link model has been developed and the equation of motion redefined to fit the external application of forces at two coordinates. This model has been used to study the gross effects of action taken b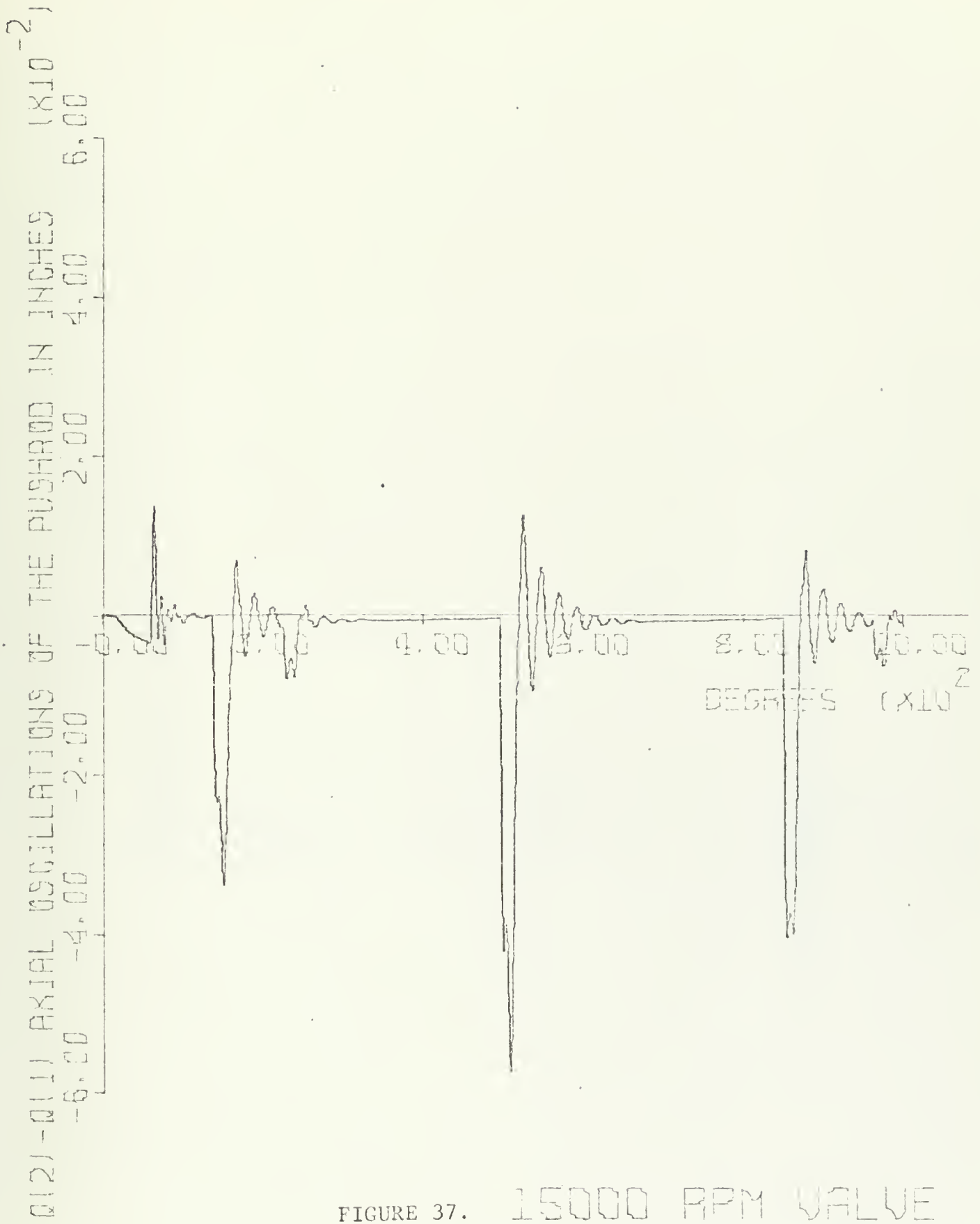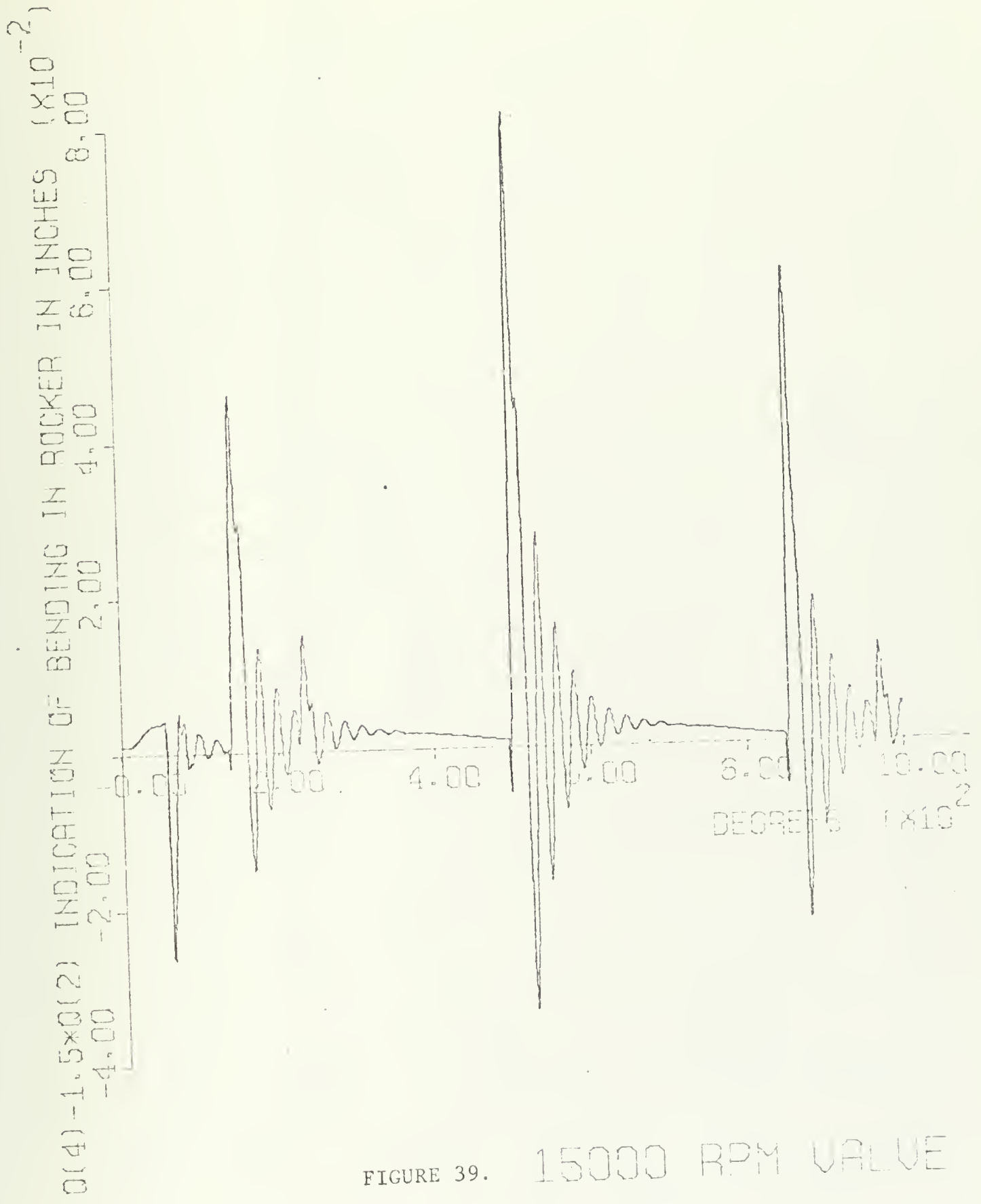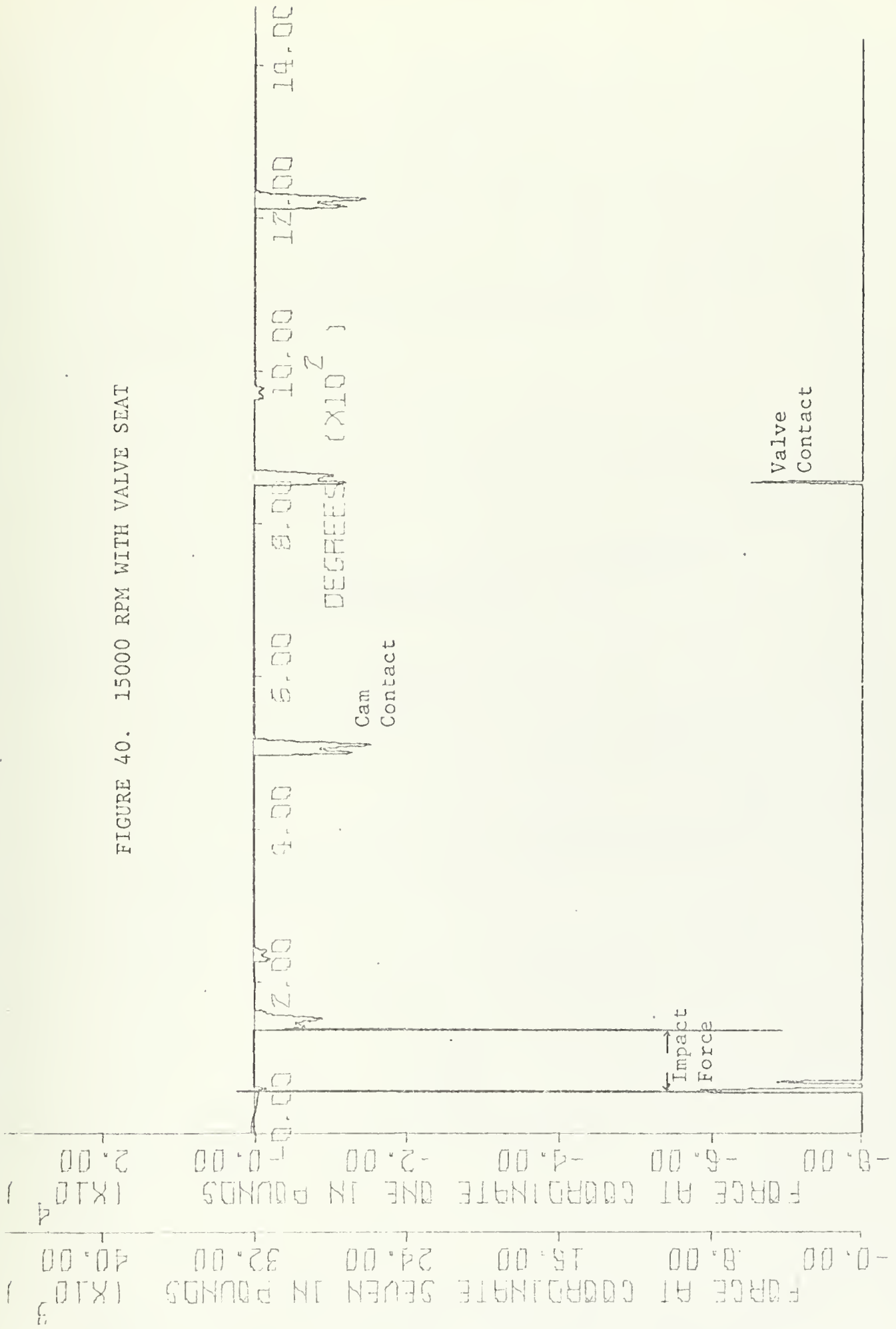y the model as it is fitted into different loading situations. The solution of the equation of motion was carried out by an integration technique.

One of the problems associated with the model as now defined is that it does not take into account the propagation velocity of elastic waves in the structure. This gives some internal disturbances due to the fact that some of the high frequency mode shapes travel faster through this mathematical model than they would through an actual model. This is best evidenced by the initial increase in force between the cam and pushrod when the valve strikes the valve seat. A computer printed output of the action at coordinate one at the moment of impact at coordinate seven shows that there is at first a reduction in F_1, but that subsequently, before the pushrod is pulled away and the force goes to zero, it increases. An examination of Figures 23 to 32 indicates an initial increase in the negative value of the F_1 curve before it is brought to zero with the separation of the cam and pushrod. This is due to the events occurring at one end being "felt" at the other end of the mechanism in one time step. The high frequency mode shapes will reach peak value in the model prior to pushrod-cam separation. This occurrence is slight and happens in a short period of time, (depending on the speed, but it is measured in milliseconds) and the overall effect of the pushrod lifting from cam surface is still not affected.

Another area of interest, which was not examined, was that of
accounting for all parts of the model separating from each other. This
would involve internal forces and would probably best be solved by
working with the element, vice the system coordinates.

The effect of clearance can be incorporated along the same lines as
mentioned above. As of now the only clearances that can be incorporated
are at coordinate one and seven.

As the model now stands it gives a good indication of the effect of
impact, machine error, cam speed, and valve placement on the action of
the different members in the system. It could be argued that some of
the forces obtained on impact would rapidly tear the mechanism apart.
There is no counter argument to this except to state that the intention
is to show the cause and immediate effect in terms of force experienced
by the system. It should be noted that all runs are at a very high
speed and therefore, subject the model to very high forces. Interpre-
tation of the large forces on impact, the oscillations of force, and
the amount of bounce of one element on another, is part of the reason
for setting up such a model.

Many of the design criteria for a good valve train have been violated
in order to demonstrate the potential of the model. The model is well
adapted to examine features that should not occur in a good valve train
and graphically demonstrates what will happen in terms of force and
displacement responses if they do occur.

The model is also extremely useful in examining a system that appears
to be operating sufficiently well. Force oscillation in high speed
mechanisms can be a problem which will not normally become evident until

77

material fatigue appears. The mechanism does not have to run improperly

to have large force oscillation. Figure 33 for the machining error

gives a good indication of this.

It is felt that the model in its present configuration can give an

overall picture of system response. With relatively slight modification

the model can be made to represent a specific mechanism and give

individual response characteristics.

MATRIX MANIPULATION OF EQUATIONS OF MOTION FOR

DIFFERENT SITUATIONS OF PROBLEM

A. CONTACT AT CAM AND CAM FOLLOWER ONLY

In the basic equations of motion

$$[m_{ij}]\{\ddot{q}_i\} + [c_{ij}]\{\dot{q}_i\} + [k_{ij}]\{q_i\} = \{F_i\} \qquad (35)$$

where (i = 1,2,...7) and (j = 1,2,...7).

F_1 is unknown and $F_2 - F_7$ are known and equal to zero. q_1, $\dot{q}_1$, and $\ddot{q}_1$, equal the value of displacement, velocity and acceleration of the cam.

Equation 35 can be expanded and partitioned to take advantage of the known values.

Expanding and partitioning Equation 35 yields,

$$
\begin{bmatrix}
m_{11} & m_{12} \text{--} m_{17} \\
m_{21} & m_{22} \text{--} m_{27} \\
\cdot & \cdot \quad\cdot \\
\cdot & \cdot \quad\cdot \\
\cdot & \cdot \quad\cdot \\
\cdot & \cdot \quad\cdot \\
m_{71} & m_{72} \text{--} m_{77}
\end{bmatrix}
\begin{Bmatrix}
\ddot{q}_1 \\
\ddot{q}_2 \\
\cdot \\
\cdot \\
\cdot \\
\cdot \\
\ddot{q}_7
\end{Bmatrix}
+
\begin{bmatrix}
c_{11} & c_{12} \text{--} c_{17} \\
c_{21} & c_{22} \text{--} c_{27} \\
\cdot & \cdot \quad\cdot \\
\cdot & \cdot \quad\cdot \\
\cdot & \cdot \quad\cdot \\
\cdot & \cdot \quad\cdot \\
c_{71} & c_{72} \text{--} c_{77}
\end{bmatrix}
\begin{Bmatrix}
\dot{q}_1 \\
\dot{q}_2 \\
\cdot \\
\cdot \\
\cdot \\
\cdot \\
\dot{q}_7
\end{Bmatrix}
+
\begin{bmatrix}
k_{11} & k_{12} \text{--} k_{17} \\
k_{21} & k_{22} \text{--} k_{27} \\
\cdot & \cdot \quad\cdot \\
\cdot & \cdot \quad\cdot \\
\cdot & \cdot \quad\cdot \\
\cdot & \cdot \quad\cdot \\
k_{71} & k_{72} \text{--} k_{77}
\end{bmatrix}
\begin{Bmatrix}
q_1 \\
q_2 \\
\cdot \\
\cdot \\
\cdot \\
\cdot \\
q_7
\end{Bmatrix}
=
$$

$$= \left\{ \begin{array}{c} F_1 \\ 0 \\ \cdot \\ \cdot \\ \cdot \\ \cdot \\ 0 \end{array} \right\} \qquad (36)$$

Removing the top equation for F_1 , Equation 36, the set of remaining equations can be written,

$$\left\{ \begin{array}{c} m_{21} \\ \cdot \\ \cdot \\ \cdot \\ m_{71} \end{array} \right\} \ddot{q}_1 + \left[\begin{array}{ccc} m_{22} & \text{---} & m_{27} \\ \cdot & & \cdot \\ \cdot & & \cdot \\ \cdot & & \cdot \\ m_{72} & \text{---} & m_{77} \end{array} \right] \left\{ \begin{array}{c} \ddot{q}_2 \\ \cdot \\ \cdot \\ \cdot \\ \ddot{q}_7 \end{array} \right\}$$

$$+ \left\{ \begin{array}{c} c_{21} \\ \cdot \\ \cdot \\ \cdot \\ c_{71} \end{array} \right\} \dot{q}_1 + \left[\begin{array}{ccc} c_{22} & \text{---} & c_{27} \\ \cdot & & \cdot \\ \cdot & & \cdot \\ \cdot & & \cdot \\ c_{72} & \text{---} & c_{77} \end{array} \right] \left\{ \begin{array}{c} \dot{q}_2 \\ \cdot \\ \cdot \\ \cdot \\ \dot{q}_7 \end{array} \right\} \qquad (37)$$

$$+ \left\{ \begin{array}{c} k_{21} \\ \cdot \\ \cdot \\ \cdot \\ k_{71} \end{array} \right\} q_1 + \left[\begin{array}{ccc} k_{22} & \text{---} & k_{27} \\ \cdot & & \cdot \\ \cdot & & \cdot \\ \cdot & & \cdot \\ k_{72} & \text{---} & k_{77} \end{array} \right] \left\{ \begin{array}{c} q_2 \\ \cdot \\ \cdot \\ \cdot \\ q_7 \end{array} \right\} = \left\{ \begin{array}{c} 0 \\ \cdot \\ \cdot \\ \cdot \\ 0 \end{array} \right\}$$

The full set of equations can be rewritten as Equation 38 and 39.

$$F_1 = \sum_{i=1}^{7} (m_{1i}\ddot{q}_i + c_{1i}\dot{q}_i + k_{1i}q_i) \qquad (38)$$

80

$$\{m_{j1}\}\ddot{q}_1 + [m_{jk}]\{\ddot{q}_j\} + \{c_{1j}\}\dot{q}_1 + [c_{jk}]\{\dot{q}_j\}$$

$$+ \{k_{1j}\}q_1 + [k_{jk}]\{q_j\} = \{0\} \tag{39}$$

where $(j = 2,3,\ldots,7)$ $(k = 2,3,\ldots,7)$.

Rearranged, Equation 39 can be rewritten as,

$$[m_{jk}]\{\ddot{q}_j\} + [c_{jk}]\{\dot{q}_j\} + [k_{jk}]\{q_j\} = \{p_j\} \tag{40}$$

where

$$\{p_j\} = - \{m_{j1}\}\ \ddot{q}_1 - \{c_{j1}\}\ \dot{q}_1 - \{k_{j1}\}\ q_1 \tag{41}$$

and $(j = 2,3,\ldots,7)$ $(k = 2,3,\ldots,7)$.

This set of equations can now be solved by the numerical integration technique outlined in Appendix B, to yield $\{\ddot{q}_j\}$, $\{\dot{q}_j\}$, $\{q_j\}$, where $(j = 2,3,\ldots,7)$. With these values and knowing $\ddot{q}_1$, $\dot{q}_1$ and q_1, F_1 can be found.

B. NO CONTACT

In this case all the forces are known to equal zero. The basic equation of motion is left as is,

$$[m_{ij}]\{\ddot{q}_i\} + [c_{ij}]\{\dot{q}_i\} + [k_{ij}]\{q_i\} = \{0\} \tag{42}$$

where $(i = 1,2,\ldots,7)$ $(j = 1,2,\ldots,7)$.

Equation 42 is solved by the technique of Appendix B to yield $\{\ddot{q}_i\}$, $\{\dot{q}_i\}$ and $\{q_i\}$ where $i = 1,2,\ldots7$.

C.   CONTACT AT THE CAM AND VALVE SEAT

The equation (35) is partitioned one step farther than for part A, for in this case F_7 is not known, but q_7 equals the value of the valve seat and $\dot{q}_7$ and $\ddot{q}_7$ equal zero. Again as in part A, $F_2 - F_6$ are known to equal zero, F_1 is unknown, and $\ddot{q}_1$, $\dot{q}_1$, and q_1 equal the values associated with the cam profile. Equations 43, 44, 45, and 46 are formed in the same manner as part A, i.e., expanding, partitioning, and rearranging Equation 35.

$$F_1 = \sum_{i=1}^{7} (m_{1i}\ddot{q}_i + c_{1i}\dot{q}_1 + k_{1i}q_i) \tag{43}$$

$$F_7 = \sum_{i=1}^{7} (m_{7i}\ddot{q}_i + c_{7i}\dot{q}_i + k_{7i}q_i) \tag{44}$$

$$[m_{jk}]\{\ddot{q}_j\} + [c_{jk}]\{\dot{q}_j\} + [k_{jk}]\{q_j\} = \{P_j\} \tag{45}$$

where $j = 2,3,\ldots6$ and $k = 2,3,\ldots6$,

and $\{P_j\} = -\{m_{j1}\}\ddot{q}_1 - \{m_{j7}\}\ddot{q}_7 - \{c_{j7}\}\dot{q}_7 - \{k_{j1}\}q_1 - \{k_{j7}\}q_7 - \{c_{j1}\}\dot{q}_1$.

$$\tag{46}$$

Again the matrix equations can be solved by the technique of Appendix B to find $\{\ddot{q}_j\}, \{\dot{q}_j\}$, and $\{q_j\}$, $(j = 2,3,\ldots,6)$. F_1 and F_7 can then be solved by Equations 43 and 44.

D. CONTACT BETWEEN VALVE AND VALVE SEAT ONLY

In this case F_7 is not known, $\ddot{q}_7$ and $\dot{q}_7$ are equal to zero and q_7 is equal to the valve position. Expanding, partitioning, and rearranging Equation 35 yields Equations 47, 48, and 49.

$$F_7 = \sum_{i=1}^{7} (m_{7i}\ddot{q}_i + c_{7i}\dot{q}_i + k_{7i}q_i) \tag{47}$$

$$[m_{jk}]\{\ddot{q}_j\} + [c_{jk}]\{\dot{q}_j\} + [k_{jk}]\{q_j\} = \{P_j\} \tag{48}$$

where $(j = 1,2,\ldots,6)$ $(k = 1,2,\ldots,6)$.

and
$$\{P_j\} = -\{m_{j7}\}\ddot{q}_7 - \{c_{j7}\}\dot{q}_7 - \{k_{j7}\}q_7 \quad . \tag{49}$$

Appendix B is used to solve the matrix equations and find $\{\ddot{q}_j\}$, $\{\dot{q}_j\}$, $\{q_j\}$, $(j = 1,2,\ldots,6)$. F_7 is then solved by Equation 47.

APPENDIX B

INTEGRATION ALGORITHM

A. DEVELOPMENT

This algorithm is developed to solve the equation of motion,

$$[M]\{\ddot{q}\} + [C]\{\dot{q}\} + [K]\{q\} = \{F\} \tag{51}$$

by using a step by step time integration technique. This involves a choice of a function to represent how the acceleration changes within the time step T.

Assume that, $\ddot{q}_i(t) = f_i(t)$ $\tag{52}$

where $i = 1$ to the degree of freedom.
$$T \leq t < T + \Delta T$$

Integrate for velocity and displacement;

$$\dot{q}_i(t) = \int f_i(t)dt + C_{Vi} = g_i(t) + C_{Vi} \tag{53}$$

$$q_i(t) = \int g_i(t) + C_{Vi}t + C_{Di} = h_i(t) + C_{Vi}t + C_{Di} . \tag{54}$$

Express $q_i(t)$, $\dot{q}_i(t)$ and $\ddot{q}_i(t)$ in terms of $\ddot{q}_i(t)$ evaluated at adjacent time step end points.

$$---/---/---/---/---/---/---$$
$$T\text{-}3 \quad T\text{-}2 \quad T\text{-}1 \quad T \quad T\text{-}1 \quad T\text{+}2 \quad T\text{+}3$$
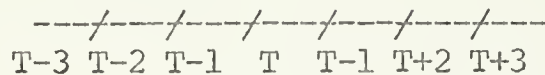
The undetermined coefficients of $f_1(t)$ are expressed in terms of acceleration values at time step end points. The results are substituted into the equation of motion. This yields an algorithm which relates values of acceleration at adjacent time steps.

84

Assume a linear acceleration function within each time step. This

yields an adaptation of Newmark's method of integration to matrix algebra.
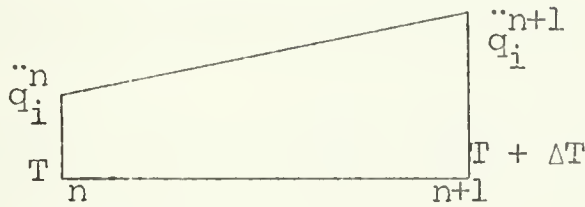
$$\text{Acceleration} = \ddot{q}_i(t) = \ddot{q}_i^n + \frac{(\ddot{q}_i^{n+1} - \ddot{q}_i^n)}{\Delta T} t \tag{55}$$

$$\text{Velocity} = \dot{q}_i(t) = \dot{q}_i^n + \ddot{q}_i^n t + \frac{(\ddot{q}_i^{n+1} - \ddot{q}_i^n)}{\Delta T} \frac{t^2}{2} \tag{56}$$

$$\text{Displacement} = q_i(t) = q_i^n + \dot{q}_i^n t + \ddot{q}_i^n \frac{2}{2} + \frac{(\ddot{q}_i^{n+1} - \ddot{q}_i^n)}{\Delta T} \frac{t^3}{6} \tag{57}$$

Evaluate $\dot{q}_i(t)$ and $q_i(t)$ at time $t = \Delta T$,

$$\dot{q}_i^{n+1} = \dot{q}_i^n + \ddot{q}_i^n \frac{\Delta T}{2} + \ddot{q}_i^{n+1} \frac{\Delta T}{2} \tag{58}$$

$$q_i^{n+1} = q_i^n + \dot{q}_i^n \Delta T + \ddot{q}_i^n \frac{(\Delta T)^2}{3} + \ddot{q}_i^{n+1} \frac{(\Delta T)^2}{6} \tag{59}$$

Let $\alpha_i^n = \dot{q}_i^n + \ddot{q}_i^n \frac{\Delta T}{2}$ \hfill (60)

and $\psi_i^n = q_i^n + \dot{q}_i^n \Delta T + \ddot{q}_i^n \frac{(\Delta T)^2}{3}$ \hfill (61)

Now $\dot{q}_i^{n+1}$ and q_i^n can be rewritten:

$$\dot{q}_i^{n+1} = \alpha_i^n + \ddot{q}_i^{n+1} \frac{\Delta T}{2} \tag{62}$$

85

$$q_i^{n+1} = \psi_i^{n+1} + \ddot{q}_i^{n+1} \frac{(\Delta T)^2}{6} \tag{63}$$

Substitute the above results for $\dot{q}_i^{n+1}$ and q_i^{n+1} into Equation 51.

$$[M]\{\ddot{q}^{n+1}\} + [C]\{\alpha^n\} + \frac{\Delta T}{2}[C]\{\ddot{q}^{n+1}\} + [K]\{\psi^n\} + \frac{(\Delta T)^2}{6}[K]\{\ddot{q}_i^{n+1}\} = \{p^{n+1}\}.$$

$$\tag{64}$$

Rearranged, $\quad \left[[M] + \frac{\Delta T}{2}[C] + \frac{\Delta T^2}{6}[K]\right]\{\ddot{q}^{n+1}\} = \{p^{n+1}\} - [C]\{\alpha^n\} - [K]\{\psi^n\}$

$$\tag{65}$$

Rewritten, $\quad [\bar{M}^{n+1}]\{\ddot{q}^{n+1}\} = \{\bar{P}^{n+1}\}$, $\tag{66}$

where $\{p^{n+1}\} = \{F\}$ evaluated at time n+1.

$$[\bar{M}^{n+1}] = [M] + \frac{\Delta T}{2}[C] + \frac{\Delta T^2}{6}[K] \tag{67}$$

$$\{\bar{P}^{n+1}\} = \{p^{n+1}\} - [C]\{\alpha^n\} - [K]\{\psi^n\} \tag{68}$$

B. ALGORITHM

1. Step 1

The initial conditions can be determined from Equation 51 evaluated at time equal to zero,

$$[M]\{\ddot{q}^0\} + [C]\{\dot{q}^0\} + [K]\{q^0\} = \{F^0\} \quad .$$

Any two of $\{\ddot{q}^0\}$, $\{\dot{q}^0\}$ or $\{q^0\}$ may be specified and the third solved for by the above equation.

2. **Step 2**

   Substitute the initial condition values into equations 60 and 61,

   $$\{\alpha_i^n\} = \{\dot{q}_i^n\} + \frac{\Delta T}{2}\{\ddot{q}_i^n\}$$

   $$\{\psi_i^n\} = \{q_i^n\} + \Delta T\{\dot{q}_i^n\} + \frac{(\Delta T)^2}{3}\{\ddot{q}_i^n\} \qquad n = 0$$

3. **Step 3**

   Set up $[\bar{M}^{n+1}]$ from Equation 67,

   $$[\bar{M}^{n+1}] = [M^n] + \frac{\Delta T}{2}[C^n] + \frac{\Delta T^2}{6}[K^n] \quad .$$

Note that $[M^n]$, $[C^n]$, and $[K^n]$ matrices may depend on motion values and this may require modification during analysis. For linear problems, i.e., this model, $[M^n]$, $[C^n]$, and $[K^n]$ remain constant and $[M]$ is only computed once.

4. **Step 4**

   Solve for $\{\bar{P}\}$ from Equation 68.

   $$\{\bar{P}_i^{n+1}\} = \{p_i^{n+1}\} - [C]\{\alpha_i^n\} - [K]\{\psi_i^n\}$$

5. **Step 5**

   From Equation 66 solve for $\{\ddot{q}_i^{n+1}\}$.

   $$\{\ddot{q}_i^{n+1}\} = [\bar{M}^{n+1}]^{-1} \quad \{\bar{P}_i^{n+1}\}$$

6. Step 6

Evaluate $\{\dot{q}^{n+1}\}$ and $\{q^{n+1}\}$ from Equations 62 and 63.

$$\{\dot{q}_i^{n+1}\} = \{\alpha_i^n\} + \{\ddot{q}_i^{n+1}\} \frac{\Delta T}{2}$$

$$\{\dot{q}_i^{n+1}\} = \{\alpha_i^{n+1}\} + \{\ddot{q}_i^{n+1}\} \frac{(\Delta T)^2}{6}$$

7. Step 7

Evaluate $\{\alpha^{n+1}\}$ and $\{\psi^{n+1}\}$ by Equations 60 and 61.

$$\{\dot{\alpha}^{n+1}\} = \{\dot{q}_i^{n+1}\} + \{\ddot{q}_i^{n+1}\} \frac{\Delta T}{2}$$

$$\{\psi^{n+1}\} = \{q_i^{n+1}\} + \{\dot{q}^{n+1}\}\Delta T + \{\ddot{q}_i^{n+1}\}\frac{(\Delta T)^2}{3}$$

8. Step 8

Let n equal n+1. Go to step 3 and reiterate for

$$\{\ddot{q}_i^{n+1}\}, \quad \{\dot{q}_i^{n+1}\} \text{ and } \{q^{n+1}\} .$$

BIBLIOGRAPHY

1. Dudley, W. M., "New Approach to Cam Design", <u>Machine Design</u>, v. 17, p. 143-148, July 1947.

2. Dudley, W. M., "New Methods in Valve Cam Design", <u>SAE Quarterly Transactions</u>, v. 2, p. 19-33, January 1948.

3. Thoren, T. R., Engemann, H. H., Stoddart, D. A., "Cam Design as Related to Valve Train Dynamics", <u>SAE Quarterly Transactions</u>, v. 6, p. 1-14, January 1952.

4. Johnson, A. R., "Motion Control for a Series System of "N" Degrees of Freedom Using Numerically Derived and Evaluated Equations", <u>Journal of Engineering for Industry</u>, v. 87, p. 191-204, May 1965.

5. Mitchell, D. B., "Cam Follower Dynamics", <u>Machine Design</u>, v. 22, p. 151-154, June 1950.

6. Mahig, J., <u>Spring and Follower Characteristics Due to Internal Damping and Cam Actuation</u>, paper presented at ASME Mechanisms Conference, Columbus, Ohio, 2-4 November 1970.

7. Rothbart, H. A., <u>Cams</u>, 1st ed., John Wiley & Sons, Inc., 1956.

8. Molian, S., <u>The Design of Cam Mechanisms and Linkages</u>, 1st ed., American Elsevier Publishing Co., Inc., 1968.

9. Shigley, J. E., <u>Mechanical Engineering Design</u>, 1st ed., McGraw-Hill Co., Inc., 1963.

10. Stoddart, D. A., "Polydyne Cam Design", <u>Machine Design</u>, v. 25, p. 121-135, January 1953.

11. Stoddart, D. A., "Polydyne Cam Design-II", <u>Machine Design</u>, v. 25, p. 146-154, February 1953.

12. Stoddart, D. A., "Polydyne Cam Design-III", <u>Machine Design</u>, v. 25, p. 149-164, March 1953.

13. Neklutin, C. N., "Designing Cam for Controlled Inertia Vibration", <u>Machine Design</u>, v. 24, p. 143-160, June 1952.

14. Molian, S., "Use of Algebraic Polynomials in Design of Cams", <u>The Engineer</u>, v. 215, p. 352-354, 22 February, 1963.

15. Neklutin, C. N., <u>Mechanisms and Cams for Automatic Machines</u>, 1st ed., Americal Elsevier Publishing Co., Inc., 1969.

16. Rahman, Z. U., and Russell, W. H., <u>An Iterative Method for Analyzing Oscillating Cam Follower Motion</u>, paper presented at ASME Conference, Columbus, Ohio, 2-4 November 1970.

17. Baranyi, S. J., _Multiple-Harmonic Cam Profiles_, paper presented at ASME Mechanisms Conference, Columbus, Ohio, 2-4 November 1970.

18. Johnson, R. C., "The Dynamic Analysis and Design of Relatively Flexible Cam Mechanisms Having More Than One Degree of Freedom", _Journal of Engineering for Industry_, v. 81, November 1959.

19. Barkan, P., "Calculation of High Speed Valve Motion With Flexible Overhead Linkage", _SAE Quarterly Transactions_, v. 61, p. 687-700, 1953.

20. Barkan, P., and McGarrity, R. V., "A Spring-Actuated, Cam-Follower System: Design Theory and Experimental Results", _Journal of Engineering for Industry_, v. 87, p. 279-286, August 1965.

21. Beggs, J. S., _Mechanisms_, McGraw-Hill Co., Inc., 1955.

22. Johnson, R. C., "Impact Forces in Mechanisms", _Machine Design_, v. 30, p. 138-146, August 1965.

23. Neklutin, C. N., "Vibration Analysis of Cams", _Machine Design_, v. 26, p. 190-198, December 1954.

24. Timoshenko, S., and Young, _Advanced Dynamics_, 1st ed., McGray-Hill Co., Inc., 1948.

25. Winfrey, R. C., _Dynamics of Mechanisms With Elastic Links_, Research and Development Division, Aerospace Group, Hughes Aircraft Co., Report No. JT 5180, March 1969.

26. Rubinstein, M. F., _Matrix Computer Analysis of Structures_, 1st ed., Prentice-Hall, Inc., 1966.

27. Timoshenko, S., and Goodier, J. N., _Theory of Elasticity_, 2nd ed., McGraw-Hill Co., Inc., New York, 1951.

28. Dubowsky, S., and Freudenstein, F., _Dynamic Analysis of Mechanical Systems With Clearances, Part I: Formation of Dynamic Model_, paper presented at ASME Mechanisms Conference, Columbus, Ohio, 2-4 November 1970.

29. Dubowsky, S., and Freudenstein, F., _Dynamic Analysis of Mechanical Systems With Clearances, Part II: Dynamic Response_, paper presented at ASME Mechanisms Conference, Columbus, Ohio, 2-4 November, 1970.

30. Hurty, W. C., and Rubinstein, M. F., _Dynamics of Structures_, 1st ed., Prentice-Hall, Inc., 1966.

INITIAL DISTRIBUTION LIST

No. Copies

1. Defense Documentation Center   2
    Cameron Station
    Alexandria, Virginia 22314

2. Library, Code 0212   2
    Naval Postgraduate School
    Monterey, California 93940

3. Professor R. C. Winfrey   6
    Department of Mechanical Engineering
    Naval Postgraduate School
    Monterey, California 93940

4. Lieutenant R. V. Andersen, USN   2
    Boston Naval Shipyard
    FPO New York City, New York

DOCUMENT CONTROL DATA - R & D

(Security classification of title, body of abstract and indexing annotation must be entered when the overall report is classified)

1 ORIGINATING ACTIVITY (Corporate author)	2a. REPORT SECURITY CLASSIFICATION
Naval Postgraduate School Monterey, California	Unclassified
	2b. GROUP

3 REPORT TITLE

Dynamic Analysis of Cams

4 DESCRIPTIVE NOTES (Type of report and, inclusive dates)

Master's Thesis; June 1971

5. AUTHOR(S) (First name, middle initial, last name)

Robert V. Andersen

6. REPORT DATE	7a. TOTAL NO. OF PAGES	7b. NO. OF REFS
June 1971	93	30

8a. CONTRACT OR GRANT NO.	9a. ORIGINATOR'S REPORT NUMBER(S)
b. PROJECT NO	
c.	9b. OTHER REPORT NO(S) (Any other numbers that may be assigned this report)
d.	

10 DISTRIBUTION STATEMENT

Approved for public release; distribution unlimited.

11. SUPPLEMENTARY NOTES	12. SPONSORING MILITARY ACTIVITY

13. ABSTRACT

This thesis deals with the computer simulated, elastic link model of an automobile cam actuated valve train. Examined are the dynamic responses to such situations as: valve bounce, pushrod bounce, excessive cam speed, cam surface machining errors, and cam profiles. The model is adaptable to various types of mechanisms and lends itself well to the incorporation on a computer graphics display.

DD FORM 1473 (PAGE 1)
1 NOV 65

S/N 0101-807-6811

Security Classification

KEY WORDS	LINK A		LINK B		LINK C	
	ROLE	WT	ROLE	WT	ROLE	WT
Cam						
Dynamic						
Valve						
Elastic Mechanisms						
Clearance						
Impact						

	LINK A		LINK B		LINK C	
	ROLE	WT	ROLE	WT	ROLE	WT

DD FORM 1473 (BACK)
1 NOV 65

S/N 0101-807-6821